Robust Design of Binary Countercurrent Adsorption Separation Processes

Giuseppe Storti
Dipartimento di Chimica Inorganica, Metallorganica e Analitica, Università degli Studi di Padova, 35131 Padova, Italy

Marco Mazzotti, Massimo Morbidelli, and Sergio Carrà
Dipartimento di Chimica Fisica Applicata, Politecnico di Milano, Piazza Leonardo da Vinci, 32, 20133 Milano, Italy

The separation of a binary mixture, using a third component having intermediate adsorptivity as desorbent, in a four section countercurrent adsorption separation unit is considered. A procedure for the optimal and robust design of the unit is developed in the frame of Equilibrium Theory, using a model where the adsorption equilibria are described through the constant selectivity stoichiometric model, while mass-transfer resistances and axial mixing are neglected.

By requiring that the unit achieves complete separation, it is possible to identify a set of implicit constraints on the operating parameters, that is, the flow rate ratios in the four sections of the unit. From these constraints explicit bounds on the operating parameters are obtained, thus yielding a region in the operating parameters space, which can be drawn a priori in terms of the adsorption equilibrium constants and the feed composition.

This result provides a very convenient tool to determine both optimal and robust operating conditions. The latter issue is addressed by first analyzing the various possible sources of disturbances, as well as their effect on the separation performance. Next, the criteria for the robust design of the unit are discussed. Finally, these theoretical findings are compared with a set of experimental results obtained in a six port simulated moving bed adsorption separation unit operated in the vapor phase.

Introduction

The possibility of separating a fluid mixture by exploiting the adsorption selectivity of a suitably chosen adsorbent solid can most conveniently be put into practice in a countercurrent apparatus based on displacement chromatography. The scheme of a true countercurrent (TCC) unit of this kind is presented in Figure 1. With reference to a binary mixture to be separated, which constitutes the feed stream to the unit, the most adsorbable component is collected from the extract stream, whereas the least adsorbable one is collected from the raffinate stream.

Since countercurrent operation technology is attractive under several aspects (cf. Ruthven, 1984), the simulated moving bed (SMB) technology has been developed in order to overcome the difficulties connected with the movement of the solid phase. In SMB units the solid beds are fixed and their continuous movement is simulated by a discrete movement obtained by shifting the feed and withdrawal points at discrete times along the column axis in the same direction as the fluid flow. In order to closely mimic the countercurrent apparatus, the four sections of the separation unit are divided in several subsections. A scheme of the SMB unit, which corresponds to the well-known Sorbex process developed by UOP (Broughton and Gerhold, 1961), is shown in Figure 2. Several applications of this process have been studied in the literature, in most cases considering units with a large number of subsections (ports) operating in the liquid phase, for example, Hashimoto et al. (1983); Ching and Ruthven (1985); Ching et al. (1985); Johnson (1989); Balannec and Hotier (1992). More recently an appli-

Correspondence concerning this article should be addressed to M. Morbidelli.

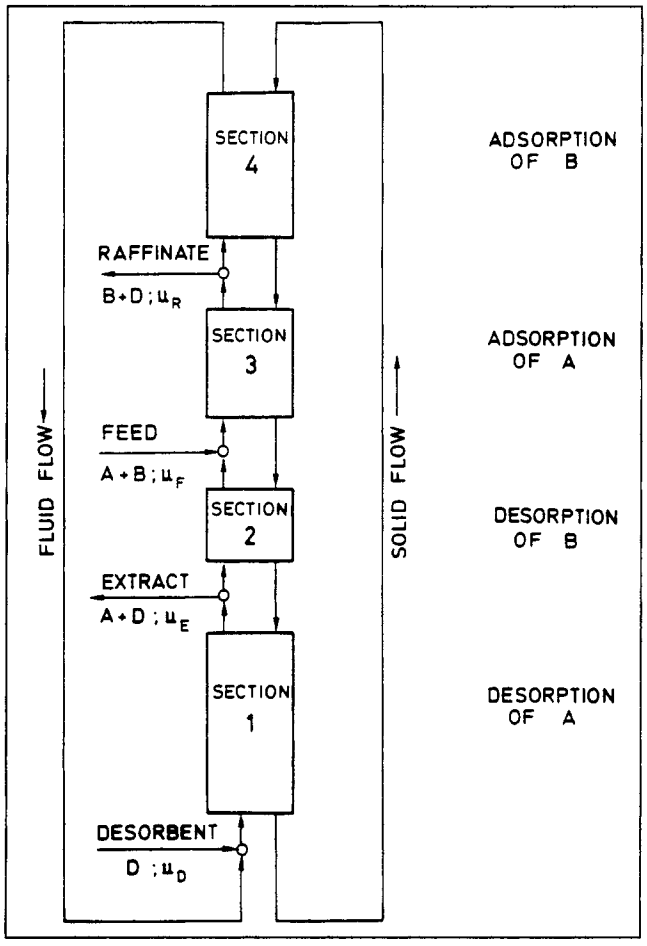

Figure 1. Four section true countercurrent (TCC) unit for adsorption separation.

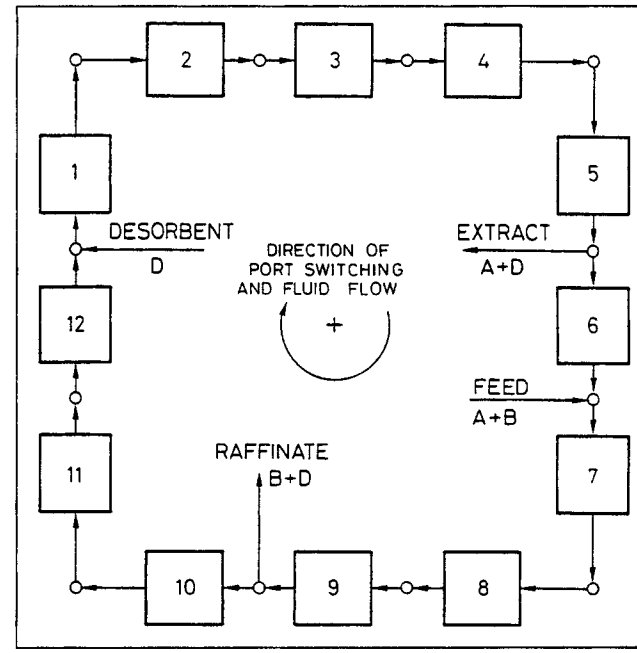

Figure 2. Simulated moving bed (SMB) unit for adsorption separation (Sorbex), having port distribution 5-1-3-3.

cation of this technology to the separation of a xylene mixture on KY Zeolites using a SMB pilot plant with only six ports and operating in the vapor phase has been reported by Storti et al. (1992).

In all cases, the equivalence between SMB and TCC units has extensively been exploited in order to model and design the adsorption separation unit (see Ruthven and Ching, 1989, for an extensive review on the subject). It must be pointed out that the stationary regime of a SMB unit is a cyclic steady state, in which each section undergoes a transient during each time period between two valve switches. It follows that the corresponding model is time dependent. On the contrary, the stationary regime of a true countercurrent apparatus is time independent, yielding a mathematical model much simpler than the previous one. Accordingly, extensive use of countercurrent models to simulate SMB units has been done (cf., Hashimoto et al., 1983; Ching and Ruthven, 1985; Storti et al., 1989).

The successful design and operation of countercurrent separation units depends upon the correct selection of the operating conditions and, in particular, of the flow rates in each section. Because of the complicated behavior of these units, such a selection is not easy and a trial-and-error procedure based on some more or less detailed model of the unit is not advisable. Accordingly, several procedures have been proposed in the literature to guide the optimal design of these units. In general, these are based on some simplified model, whose solution provides explicit expressions for the optimal operating parameters. Some of these earlier procedures, based on the approximation of the unit as a sequence of stages and then on the application of a McCabe-Thiele-like analysis, have been reviewed by Ruthven (1984), and used by Ching et al. (1985). An alternative approach is based on the equilibrium theory model which takes into account the nonlinearity of the adsorption equilibrium isotherm, whereas it neglects the effect of axial mixing and mass transport resistances (Storti et al., 1989). This model has provided a very useful tool for the qualitative simulation of countercurrent separation units, since in many applications the unit behavior is mostly determined by the properties of the adsorption equilibria.

With reference to the generic jth section shown in Figure 3 and considering a binary system (besides the desorbent), the equilibrium theory model is constituted of the following set of first-order hyperbolic partial differential equations:

$$\frac{\partial}{\partial \tau}\left[\epsilon^* y_i^j + (1-\epsilon^*)\sigma\theta_i^j\right] + (1-\epsilon_p)\sigma\frac{\partial}{\partial x}\left[m_j y_i^j - \theta_i^j\right] = 0 \qquad (i=1, \ldots, NC), \quad (1)$$

where

$$\theta_i^j = f_i^{eq}(y^j) \quad (i=1, \ldots, NC), \qquad (2)$$

with boundary conditions:

$$y_i^j(\tau, 0) = (y_i^j)^a \quad (i=1, \ldots, NC)$$

$$\theta_i^j(\tau, 1) = (\theta_i^j)^b \quad (i=1, \ldots, NC)$$

$$y_i^j(0, x) = (y_i^j)^o \quad (i=1, \ldots, NC), \qquad (3)$$

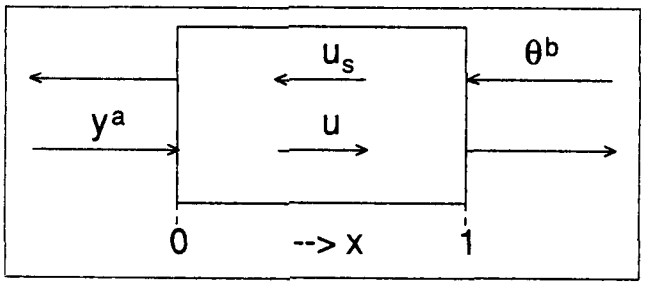

Figure 3. Generic section of a true continuous countercurrent unit.

where y_i and θ_i represent the fluid and adsorbed phase concentrations, respectively, while all the other quantities are defined in the Notation. It is worth noticing the different formulation of Eqs. 1 to 3 with respect to Eqs. 1 to 6 in Storti et al., (1989), where a minor error in the position of one of the BC's was present: in that article the condition $\zeta = 1$ should read $\zeta = 1/(1-\mu_j\epsilon_p)$, wherever it appears.

In the case of a countercurrent unit with four sections (that is, $j = 1, \ldots, 4$), four systems of equations, as Eqs. 1 to 3 above, must be considered, together with boundary conditions that take into account the proper links between neighboring columns. From the equations above it is readily seen that as far as steady-state conditions are concerned, the key design parameters as determined by equilibrium theory are the net mass flow rate ratios m_j, defined as the ratio between the net fluid mass flow rate and the adsorbed phase mass flow rate in each section of the unit:

$$m_j = \frac{\text{net fluid flow rate}}{\text{adsorbed phase flow rate}} = \frac{u_j\rho_f - u_s\epsilon_p\rho_f}{u_s\rho_s\Gamma^\infty(1-\epsilon_p)}, \tag{4}$$

where the net fluid flow rate is evaluated as the difference between the fluid flow rate and the backmixed portion of it, due to the fluid carried by the solid inside the macropores. The design problem is then reduced to the estimation of the m_j values which optimize the separation performance. In particular, in the next section we illustrate the procedure for estimating the m_j values which lead to complete separation.

Complete Separation Operating Conditions

In a four section countercurrent adsorption separation unit, the conditions to be imposed on the operating parameters in order to achieve complete separation of the feed components can be easily expressed in terms of the net flow rates of the components to be separated in each section of the unit. The net flow rate of the ith component in the jth section is proportional to the quantity f_i^j, given by $f_i^j = m_j y_i^j - \theta_i^j$. To achieve complete separation of a three-component system, the net flow rates of component A, the most adsorbable one, must be such that it is conveyed to the extract outlet, whereas component B, the least adsorbable one, must be conveyed to the Raffinate outlet (cf. Ching et al., 1985) (see Figure 1). From these considerations and the definition of f_i^j, it is seen that in terms of net flow rate ratios the following conditions must be fulfilled:

$$\begin{aligned}
&\text{Section 1:} && m_1 > \theta_A^1/y_A^1,\ m_1 > \theta_B^1/y_B^1\\
&\text{Section 2:} && \theta_B^2/y_B^2 < m_2 < \theta_A^2/y_A^2\\
&\text{Section 3:} && \theta_B^3/y_B^3 < m_3 < \theta_A^3/y_A^3\\
&\text{Section 4:} && m_4 < \theta_A^4/y_A^4,\ m_4 < \theta_B^4/y_B^4.
\end{aligned} \tag{5}$$

In the case of a linear adsorption isotherm, $\theta_i = K_i y_i$, the above conditions can readily be made explicit, so as to obtain the following constraints on the net flow rate ratios:

$$\begin{aligned}
&K_A < m_1 < \infty\\
&K_B < m_2 < K_A\\
&K_B < m_3 < K_A\\
&\frac{-\epsilon_p}{\sigma(1-\epsilon_p)} < m_4 < K_B.
\end{aligned} \tag{6}$$

These inequalities define a region in the four-dimensional space having the operating parameters m_1, m_2, m_3 and m_4 as coordinates, whose points represent operating conditions corresponding to complete separation. It is noteworthy that these conditions, and therefore the mentioned domain, depend neither on the composition of the feed to be separated nor on the adsorptivity of the desorbent.

Let us consider the two central sections of the Sorbex unit, which have a crucial role in the separation performance of the unit. Since m_3 must be greater than m_2, so as to have a positive feed flow rate, the constraints (Eq. 6) on m_2 and m_3 can be rewritten as follows:

$$K_B < m_2 < m_3 < K_A. \tag{7}$$

These inequalities define the projection onto the $m_2 - m_3$ plane of the four-dimensional region of complete separation mentioned above. It is worth noticing that the obtained projection is particularly useful for applications since it does not depend on the net flow rate ratios in sections 1 and 4. Accordingly, it can be concluded that any pair of $m_2 - m_3$ values which lies within the triangular region in the $m_2 - m_3$ plane in Figure 4 leads, in the framework of equilibrium theory, to complete separation performance.

The usefulness of relationships (Eq. 6) above, particularly in bulk separation processes, is limited by the presence of two phenomena, that is, the competition towards adsorption among the species in the fluid phase and the limitation of the overall adsorbable mass, when the adsorbent approaches saturation conditions. Both these phenomena are ignored by the linear equilibrium model, whereas a much better description is offered by the so called constant selectivity, stoichiometric model:

$$\theta_i = \frac{K_i y_i}{\sum_{j=1}^{NC} K_j y_j}. \tag{8}$$

Using the nonstoichiometric version of the constant selectivity model—where a further term equal to one appears in the denominator—Rhee et al. (1971), have obtained the analytic solution of the single section model in Eqs. 1 to 3. This important result provides the basis for all the design procedures for countercurrent units to be described in the following.

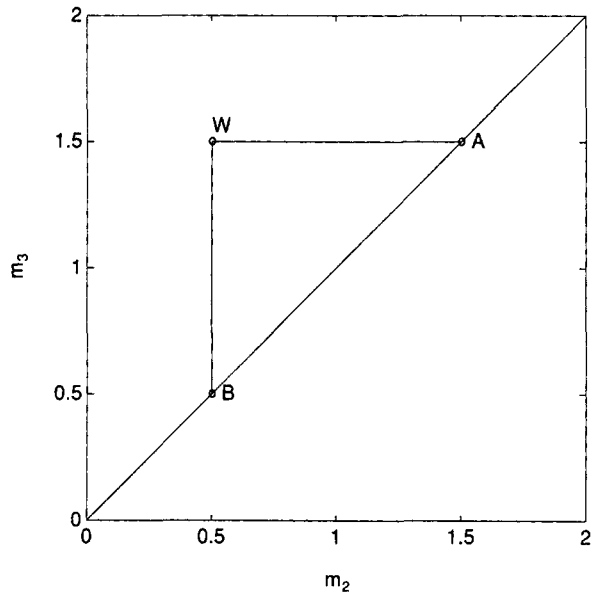

Figure 4. Complete separation region in the $m_2 - m_3$ plane for a linear system: $K_A = 1.5$, $K_B = 0.5$.

In particular, with reference to the equilibrium model (Eq. 8), Storti et al. (1989), have developed the analytical expressions of the boundaries of the region in the m-space corresponding to complete separation operation. Contrary to Eqs. 6 and 7 these expressions are reported in implicit form, that is, the boundaries depend not only on the equilibrium parameters but also on the net flow rate ratios in the neighboring sections. As a consequence the shape of the complete separation region in the $m_2 - m_3$ plane is expected to become more complex than the single triangle shown in Figure 4.

The aim of this work is to derive explicit expressions for the boundaries of the complete separation region in the $m_2 - m_3$ plane in the case where the constant selectivity, stoichiometric model (Eq. 8) is considered. Our analysis is limited to the case of binary separation, that is, three-component systems, in which the desorbent has intermediate adsorptivity with respect to those of the two components to be separated. Nevertheless, this is the case of greatest applicative interest. The results we present require some mathematical derivations in the framework of Equilibrium Theory, which might be of limited interest from the strict engineering point of view. Therefore, they have been condensed and the important details have been confined in the Appendices at the end of the article. Mathematical details of the derivations are provided in the third and sixth sections. In the subsequent sections, the final relationships for optimal and robust design of the unit are reported and their application is discussed in connection with the operation of a SMB pilot plant.

It is worth stressing that the obtained result is very useful in applications when dealing with these complicated separation units. Namely, the possibility of *a priori* drawing the region of complete separation allows us not only to avoid a rather cumbersome trial-and-error design procedure but also to address the important issue of *design robustness*. By this we mean the ability of the designed unit to keep operating within the region of optimal separation, even though the system characteristics change in time with respect to the original nominal values. This may be the consequence of changes in the properties of the adsorption system due to the aging of the adsorbent, or it may originate from a poor control of the operating conditions, for example, the flow rates of the relevant streams. A clear and explicit knowledge of the complete separation region allows us to locate the operating conditions of the unit sufficiently away from the critical boundaries so that its performance remains satisfactory (that is, corresponding to complete separation) even in the presence of the system disturbances mentioned above.

Single Section

With reference to Storti et al. (1989), we report in the following the solution of the problem in Eqs. 1 to 3 in terms of the steady-state concentration profiles in a single column for a three component system.

For three-component stoichiometric systems the theory establishes a one-to-one mapping between the space of fluid or solid concentrations, y or θ, and a two-dimensional space whose coordinates are two positive real parameters, Ω_1 and Ω_2. Given an adsorbed phase composition, or the corresponding equilibrium fluid phase composition, the Ω values are obtained as roots of the following quadratic equation:

$$\sum_{i=1}^{3} \frac{\theta_i}{K_i - \Omega} = 0, \tag{9}$$

which can be rewritten in terms of fluid phase concentrations as:

$$\sum_{i=1}^{3} \frac{K_i y_i}{K_i - \Omega} = 0. \tag{10}$$

It follows that the fluid phase and the corresponding equilibrium adsorbed phase have different compositions, but they share the same pair of Ω values.

Both the concentration space and the space Ω have dimension two, since the concentrations of only two components, A and B, are enough to fully characterize a stoichiometric system. If the lth component is not present in the state under consideration, that is, $\theta_l = 0$, then Eq. 9 becomes a linear equation with only one root and the other Ω value is given by K_l. Furthermore, since the following inequalities hold:

$$K_B \le \Omega_1 \le K_D \le \Omega_2 \le K_A, \tag{11}$$

the space of the Ω values can be seen as the set of ordered pairs (Ω_1, Ω_2), with $0 < \Omega_1 < \Omega_2$.

Equation 9 produces the Ω values for a given composition, whereas the inverse relationships, which give the concentrations in terms of the Ω pair, are given by the following relationships (Rhee et al., 1989; Storti et al., 1989):

$$\theta_A = \frac{(K_A - \Omega_2)(K_A - \Omega_1)}{(K_A - K_B)(K_A - K_D)}$$

$$\theta_B = \frac{(K_B - \Omega_2)(K_B - \Omega_1)}{(K_B - K_A)(K_B - K_D)}$$

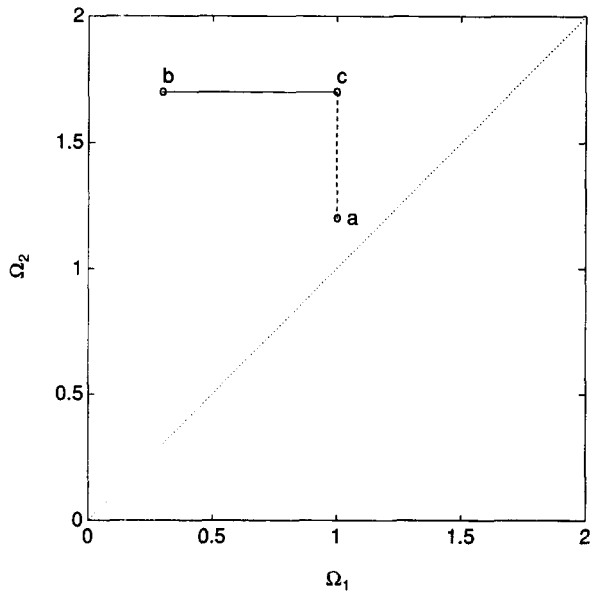

Figure 5. Solution in the $\Omega_1 - \Omega_2$ plane of a single section, 3-component system: (a) inlet fluid state; (b) inlet solid state; (c) intermediate state; — simple wave transition; —— shock wave transition.

$$y_A = \theta_A \frac{K_B K_D}{\Omega_2 \Omega_1}$$

$$y_B = \theta_B \frac{K_A K_D}{\Omega_2 \Omega_1}. \tag{12}$$

The motivation for introducing the space Ω is that the complete solution of the problem under examination can be obtained most conveniently in terms of Ω values. In the physical space $x-\tau$, the solution is constituted of a number of constant states separated by transitions, which can be continuous (called simple waves) or discontinuous (called shock waves). Only one Ω value can change across each transition, and whether it increases or decreases through it determines the character of the transition itself.

Given the inlet fluid phase and adsorbed phase compositions (y_i^a and θ_i^b in Eq. 3 and in Figure 3) two points in the space Ω are obtained with coordinates (Ω_1^a, Ω_2^a) and (Ω_1^b, Ω_2^b). These are shown in Figure 5 together with the point representing the intermediate state $c(\Omega_1^a, \Omega_2^b)$. The two segments $b-c$ and $c-a$ have the transitions connecting the three states mentioned above as counterparts in the physical space. The transition between state a and state c is a shock wave if $\Omega_2^b > \Omega_2^a$ and a simple wave if $\Omega_2^b < \Omega_2^a$; the transition between state c and state b is a shock wave if $\Omega_1^b > \Omega_1^a$ and a simple wave if $\Omega_1^b < \Omega_1^a$. After the completion of the transient, the fluid and adsorbed phases, in equilibrium with each other, exhibit constant composition in the entire column. This corresponds to a constant state in the space Ω, which can be selected by a proper choice of the flow rate ratio m as follows:

- The inlet fluid state a characterized by the Ω pair (Ω_1^a, Ω_2^a).
- The intermediate constant state c characterized by the Ω pair (Ω_1^a, Ω_2^b).
- The inlet solid state b with the Ω values (Ω_1^b, Ω_2^b).
- The state (Ω_1^a, Ω), with $(\Omega_2^b < \Omega < \Omega_2^a)$, if the transition $c-a$ is a simple wave.
- The state (Ω, Ω_2^b), with $(\Omega_1^b < \Omega < \Omega_1^a)$, if the transition $b-c$ is a simple wave.

The analytical relationships for the boundaries of the regions of m values producing the different constant states above are discussed in detail by Rhee et al. (1971) and by Storti et al. (1989). Once the constant state present in the column is known, the compositions of the two outlet streams are determined by single component material balances at the right and left ends of the column. By doing so, we allow the appearance of a discontinuity at either end, which is called boundary discontinuity (Rhee et al., 1971). It is also worth pointing out that the solid and fluid streams at the same end of the column are not at equilibrium, being related only by a conservation law.

We can now introduce the following result, which can be stated for a generic NC-component system and which is needed in the following:

Theorem 1. Let us consider a NC-component stoichiometric system and let Ω^a and Ω^b be the (NC-1)-dimensional vectors characterizing the composition of the fluid and solid streams entering a countercurrent adsorption column.

The components of the Ω vectors characterizing the states corresponding to the two outgoing fluid and solid streams and the constant state inside the column at steady-state conditions are such that:

$$\min\{\Omega_i^a, \Omega_i^b\} \le \Omega_i \le \max\{\Omega_i^a, \Omega_i^b\} \quad (i = 1, \ldots, NC-1). \tag{13}$$

Furthermore, if the constant state corresponding to the inlet stream at one end of the column and the one prevailing inside the column at steady state have one of the elements of the corresponding Ω vectors which are equal, say Ω^*, then Ω^* is also one of the components of the Ω vector characterizing the outlet stream at the same end of the column.

The proof of this theorem is given in Appendix A.

The Four-Section Countercurrent Separation Unit

A schematic representation of the four-section countercurrent separation unit under the requirement of complete separation can be given in terms of the Ω values characterizing each stream, as shown in Figure 6. Notice that the pure desorbent stream is characterized by the pair (K_B, K_A) and that, according to the condition in Eq. 11, the state corresponding to the Extract is characterized by $\Omega_1 = K_B$, while the one corresponding to the Raffinate is characterized by $\Omega_2 = K_A$. In the feed stream, the desorbent is absent, hence one of the Ω values must be equal to K_D. The other Ω value is obtained by solving Eq. 10 with $y_i = y_i^F$, that is:

$$\Omega_F = \frac{K_A K_B}{K_A y_A^F + K_B y_B^F} \tag{14}$$

which can be either smaller or greater than K_D.

We can now proceed to identify the pair (Ω_1, Ω_2), indicated in Figure 6 for each section of the unit, which corresponds to the constant state prevailing in the section at steady state. As

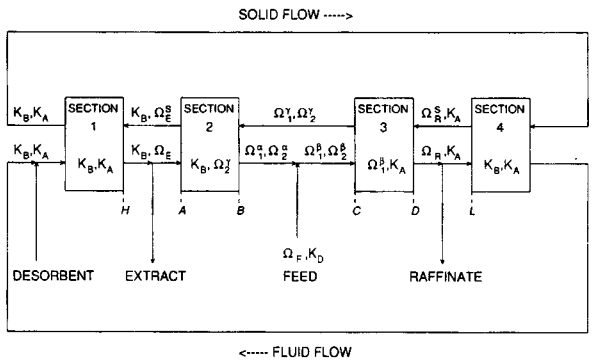

Figure 6. Four section separation unit, with the indication of the Ω values satisfying the necessary and sufficient conditions to fulfill the requirement of complete separation.

mentioned above, the specific values of the Ω parameters depend upon the value of the flow rate ratio in each section. However, a limitation of general validity on the range of the admittable Ω values inside the four section separation unit is given by the following theorem, which, similarly to theorem 1, is proved for a *NC*-component system in Appendix B.

Theorem 2. Let us consider the NC-component feed and desorbent streams entering a four section unit and let Ω^F *and* Ω^D *be the* $(NC-1)$*-dimensional vectors characterizing the composition of the two streams.*

Whatever the compositions of the two streams are, it follows that every state that can be achieved within the four section separation unit at steady-state conditions (including the outgoing Extract and Desorbent streams) is characterized by a set of Ω *values such that:*

$$\min\{\Omega_i^f, \Omega_i^D\} \le \Omega_i \le \max\{\Omega_i^F, \Omega_i^D\} \quad (i=1, \ldots, NC-1). \quad (15)$$

Thus Eq. 15 allows us to identify, based only on the compositions of the two incoming streams, a region in the Ω space which must contain all the points characterizing the composition of the states in the unit. In the particular case of a three-component system, it follows that all the states present in the unit are represented by points lying within the rectangle with vertices F and D in the plane $\Omega_1-\Omega_2$, shown in Figures 7a and 7b in the case where $\Omega_F<K_D$ or $\Omega_F>K_D$, respectively. The dashed area in the same figures represent points corresponding to states that, according to this theorem, cannot be reached by the streams within the separation unit, even though they fulfill the inequalities in Eq. 11 deriving from their definition.

We can now determine the states in the four sections compatible with the requirement of complete separation operation, as shown in Figure 6. This further reduction of the region of admittable states previously determined through Eq. 15 is due to the interaction among the four columns. In particular, the following complete separation proposition is proved in Appendix C for a three-component stoichiometric system with an intermediate desorbent:

Theorem 3 (Complete Separation Proposition). Necessary and sufficient condition to obtain complete separation is that the constant states prevailing in each section are those reported

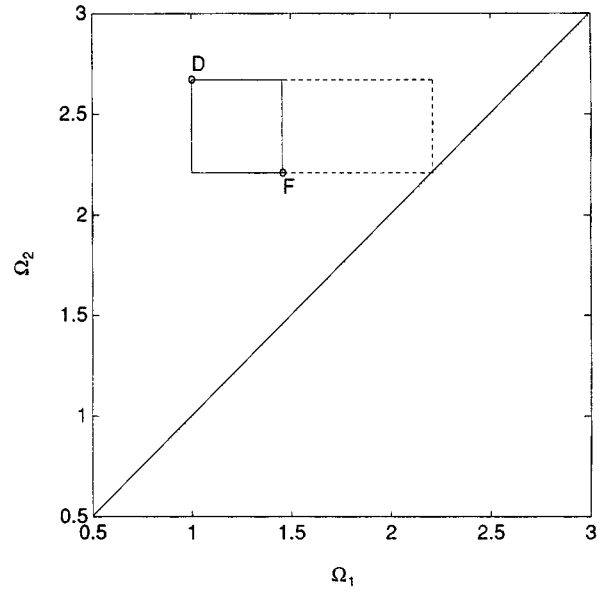

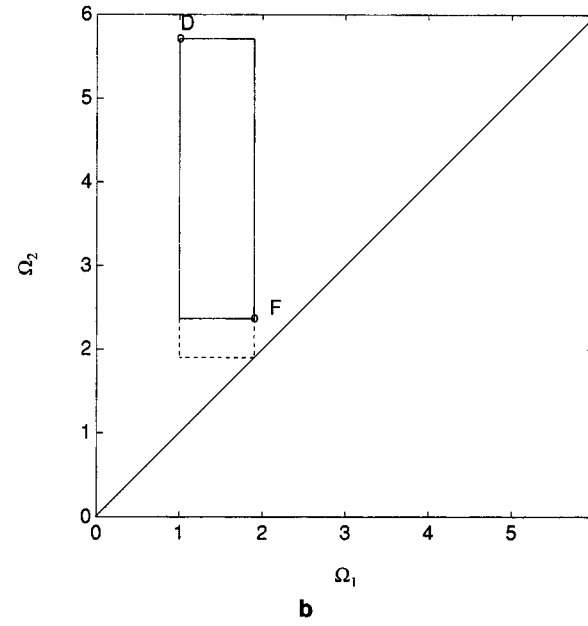

Figure 7. Region of accessible states in the $\Omega_1-\Omega_2$ plane for a four section separation unit: (a) $\Omega_F<K_D$; $K_A=2.67$, $K_B=1$, $K_D=2.21$, $y_A^F=0.5$, $y_B^F=0.5$, $\Omega_F=1.46$; (b) $\Omega_F>K_D$; $K_A=5.71$, $K_B=1$, $K_D=1.9$, $y_A^F=0.3$, $y_B^F=0.7$, $\Omega_F=2.37$; (cf. Storti et al., 1989).

in the first column of Table 1, with the relevant Ω *values as in columns 2 and 3.* Ω_1^β *and* Ω_2^γ *are as yet undetermined values, which satisfy the conditions (after theorem 2):*

$$K_B \le \Omega_1^\beta \le \min\{K_D, \Omega_F\} \le \max\{K_D, \Omega_F\} \le \Omega_2^\gamma \le K_A, \quad (16)$$

To obtain the desired constant states in each section, the corresponding net flow rate ratios have to satisfy the specific conditions reported in the last column of Table 1.

Table 1. Necessary and Sufficient Conditions for Complete Separation

Section	State	Ω_1	Ω_2	m range
1	fluid	K_B	K_A	$\frac{K_A}{K_D} < m_1 < +\infty$
2	intermediate	K_B	Ω_2^γ	$\frac{\Omega_2^\gamma \Omega_1^\gamma}{K_A K_D} < m_2 < \frac{(\Omega_2^\gamma)^2}{K_A K_D}$
3	intermediate	Ω_1^β	K_A	$\frac{(\Omega_1^\beta)^2}{K_B K_D} < m_3 < \frac{\Omega_2^\beta \Omega_1^\beta}{K_B K_D}$
4	solid	K_B	K_A	$\frac{-\epsilon_p}{\sigma(1-\epsilon_p)} < m_4 < \frac{K_B}{K_D}$

It is worth pointing out the substantial simplification introduced by this result into the analysis of the four-section separation unit. In particular, it is important to stress that in each column of the unit only one, among the different possible steady-state regimes described in the previous section, is compatible with the requirement of complete separation, and as a consequence the corresponding range for the net flow rate ratio is also unique.

Moreover, from Table 1 we notice that the hypothesis of theorem 1 are fulfilled in the first section where Ω_2 is equal to Ω_2^γ, which characterizes the composition of the inlet adsorbed phase. Similarly, the element Ω_1 corresponding to the state prevailing in the third section is equal to Ω_1^β, which characterizes the composition of the inlet fluid stream. Thus, by applying the conclusion of theorem 1 together with the constraint in Eq. 15, the following relationships are obtained:

$$\Omega_2^\alpha = \Omega_2^\gamma, \tag{17}$$

$$\Omega_1^\gamma = \Omega_1^\beta. \tag{18}$$

The Design Problem: Complete Separation under Robust Operation

It has been shown by Storti et al. (1989), that the overall and the single component material balances at the nodes of the unit, together with the single component material balances at each end of the four sections, characterize the steady-state behavior of the unit by leaving four degrees of freedom. In order to fully determine the system the most natural choice is to assign the flow rate ratio in the four sections of the unit. Accordingly, the simulation problem, that is, the question of how the system behaves given certain operating conditions, can be solved in the most general case. The only requirement is that the assigned operating conditions fulfill the trivial physical constraints, namely that all the flow rates are positive.

In principle the design problem, that is, the problem of determining the operating conditions to obtain a desired separation performance, can be tackled by solving several simulation problems within a trial-and-error procedure, until the design requirements are fulfilled. The flow rate ratios are the most natural design parameters, as well as the correct control variables, since they can be easily controlled by manipulating one internal flow rate (for example, the flow rate in the first section) and the flow rates of three among the four inlet and outlet streams. This choice makes the system constituted of the overall material balances at the nodes of the unit fully determined. An example of the experimental implementation of this control strategy has been reported by Storti et al. (1992), with reference to a Simulated Moving Bed adsorption separation pilot plant operated in the vapor phase.

In this work, an explicit solution of the design problem is developed. For the binary system under examination, the requirement of complete separation together with the results of Equilibrium Theory has led to the scheme shown in Figure 6, with the constraints on the flow rate ratios m_1, m_2, m_3, m_4, given by the inequalities in Table 1. In the figure, eight unknown Ω values are still present: Ω_2^γ, Ω_1^γ, Ω_1^α, Ω_2^β, Ω_E, Ω_E^S, Ω_R, Ω_R^S. Furthermore, eight flow rate ratios must be determined: the four design parameters m_1, m_2, m_3, m_4, and the fluid flow rates of the Feed, fresh Desorbent, Extract and Raffinate streams. These unknowns are connected by 12 overall and single component material balances at the two ends of the sections whose labels are indicated in Figure 6, and at the nodes of the unit.

A proper selection of these 12 material balances leads to the following set of equations:

- Overall material balances at each node of the unit:

$$\frac{1}{\mu_D} = \frac{1}{\mu_1} - \frac{1}{\mu_4} \tag{19}$$

$$\frac{1}{\mu_E} = \frac{1}{\mu_1} - \frac{1}{\mu_2} \tag{20}$$

$$\frac{1}{\mu_F} = \frac{1}{\mu_3} - \frac{1}{\mu_2} \tag{21}$$

$$\frac{1}{\mu_R} = \frac{1}{\mu_3} - \frac{1}{\mu_4} \tag{22}$$

- Overall material balances of components A and B:

$$\frac{1}{\mu_F} y_A^F = \frac{1}{\mu_E} y_A^E \tag{23}$$

$$\frac{1}{\mu_F} y_B^F = \frac{1}{\mu_R} y_B^R \tag{24}$$

- Material balance of component A at boundary H:

$$y_A^E = \mu_1[\epsilon_p y_A^{ES} + (1-\epsilon_p)\sigma\theta_A^{ES}] \tag{25}$$

- Material balance of component B at boundary L:

$$y_B^R = \mu_4[\epsilon_p y_B^{RS} + (1-\epsilon_p)\sigma\theta_B^{RS}] \tag{26}$$

- Material balance of component A at boundary A:

$$y_A^E - y_A^2(1-\epsilon_p\mu_2) = \mu_2[\epsilon_p y_A^{ES} + (1-\epsilon_p)\sigma(\theta_A^{ES} - \theta_A^2)] \tag{27}$$

- Material balance of component B at boundary D:

$$y_B^R - y_B^3(1-\epsilon_p\mu_3) = \mu_3[\epsilon_p y_B^{RS} + (1-\epsilon_p)\sigma(\theta_B^{RS} - \theta_B^3)] \tag{28}$$

• Material balance of component B at boundary B:

$$y_B^{\alpha} = \mu_2[\epsilon_p y_B^{\gamma} + (1-\epsilon_p)\sigma\theta_B^{\gamma}] \tag{29}$$

• Material balance of component A at boundary C:

$$y_A^{\beta} = \mu_3[\epsilon_p y_A^{\gamma} + (1-\epsilon_p)\sigma\theta_A^{\gamma}] \tag{30}$$

In the above equations the superficial flow rate ratio $\mu_j = u_s/u_j$ has been used. This is directly related to the design parameter m_j through the following relationship derived from Eq. 4:

$$m_j = \frac{1}{\sigma(1-\epsilon_p)}\left(\frac{1}{\mu_j} - \epsilon_p\right). \tag{31}$$

It is worth pointing out that since the above equations have been formulated assuming explicitly complete separation for the unit, they hold true only for net flow rate ratios m_j which satisfy the constraints reported in Table 1, that is, the necessary and sufficient conditions for complete separation as given by theorem 3.

Let us consider the constraints in Table 1 in detail. The bounds on m_1 and m_4 are explicit, that is, they do not depend on the other flow rate ratios. Hence the choice of the operating values of m_1 and m_4 to obtain complete separation is trivial. On the contrary, the bounds on m_2 and m_3 are given in terms of Ω values (Ω_2^{γ}, Ω_1^{γ}, Ω_2^{β}) that are obtained as solutions of the system in Eqs. 19-30. Thus, in principle these are functions of the flow rate ratios in all the sections of the unit and therefore the conditions on m_2 and m_3 are implicit. In the next sections, we show that the bounds on m_2 and m_3 are indeed implicit, but they are independent of m_1 and m_4. Hence, we can rearrange the system of Eqs. 19 to 30 in order to make the constraints on m_2 and m_3 explicit and then determine the region of complete separation operating conditions in the $m_2 - m_3$ plane.

The Solution of the Design Problem

In this section, we first derive explicit relationships among the unknown Ω values and the design parameters m_1, m_2, m_3 and m_4. Next, these are substituted in the inequalities reported in Table 1, which define the conditions for complete separation, so as to obtain a set of inequalities among the design parameters alone (that is, not involving the Ω values). In particular, we are concerned with the two implicit constraints in Table 1:

$$\frac{\Omega_2^{\gamma}\Omega_1^{\gamma}}{K_A K_D} < m_2 < \frac{(\Omega_2^{\gamma})^2}{K_A K_D} \tag{32}$$

$$\frac{(\Omega_1^{\gamma})^2}{K_B K_D} < m_3 < \frac{\Omega_2^{\beta}\Omega_1^{\gamma}}{K_B K_D} \tag{33}$$

where Eq. 18 has been used.

Let us begin by rearranging the original system of equations to reduce it to a simpler form. Using Eqs. 20 to 22 and 31, the external superficial flow rate ratios can be written in terms of the design parameters m_j as follows:

$$\frac{1}{\mu_F} = \sigma(1-\epsilon_p)(m_3 - m_2),$$

$$\frac{1}{\mu_E} = \sigma(1-\epsilon_p)(m_1 - m_2),$$

$$\frac{1}{\mu_R} = \sigma(1-\epsilon_p)(m_3 - m_4). \tag{34}$$

On the other hand Eq. 27, after eliminating y_A^E, y_A^{ES} and θ_A^{ES} by substituting Eqs. 23 and 25 using Eqs. 34, reduces to:

$$\theta_A^2 - m_2 y_A^2 = (m_3 - m_2) y_A^F. \tag{35}$$

Similarly, using Eqs. 24, 26, and 34, Eq. 28 leads to:

$$m_3 y_B^3 - \theta_B^3 = (m_3 - m_2) y_B^F. \tag{36}$$

These two equations can be written in the Ω space by using the relationships in Eq. 12 as well as the results reported in Table 1, so as to obtain two one-variable quadratic equations in the unknowns Ω_1^{γ} and Ω_2^{γ}:

$$(\Omega_1^{\gamma})^2 - b_1\Omega_1^{\gamma} + c_1 = 0, \tag{37}$$

$$(\Omega_2^{\gamma})^2 - b_2\Omega_2^{\gamma} + c_2 = 0, \tag{38}$$

where the coefficients are given in terms of the design parameters m_2 and m_3, the feed composition, y_i^F, and the equilibrium constants as follows:

$$b_1 = K_B + K_D m_3 - (K_D - K_B) y_B^F (m_3 - m_2), \tag{39}$$

$$c_1 = K_B K_D m_3, \tag{40}$$

$$b_2 = K_A + K_D m_2 - (K_A - K_D) y_A^F (m_3 - m_2), \tag{41}$$

$$c_2 = K_A K_D m_2. \tag{42}$$

Notice that b_1, c_1 and c_2 are positive. Moreover, since by definition of the parameters Ω we are only interested in cases where Eqs. 37 and 38 have real and positive roots, it can be concluded that also b_2 and the discriminants of the two equations should be positive. Finally, it is readily seen that the following relationships between the roots of Eqs. 37 and 38 hold true:

$$\Omega_1^{\oplus}\Omega_1^{\ominus} = K_B K_D m_3, \tag{43}$$

$$\Omega_2^{\oplus}\Omega_2^{\ominus} = K_A K_D m_2, \tag{44}$$

where we define the roots so that $\Omega_2^{\oplus} \geq \Omega_2^{\ominus}$ and $\Omega_1^{\oplus} \geq \Omega_1^{\ominus}$ and we omit the superscript γ for brevity.

It is worth noticing that, from the physical point of view, the result obtained above of separating the two unknowns Ω_2^{γ}

and Ω_1^γ in the two Eqs. 37 and 38, respectively, comes directly from the enforced requirement of complete separation. This is the condition that eliminates the component A from the Raffinate zone and the component B from the Extract zone, so making their overall material balances in Eqs. 23 and 24 so simple. Another consequence of the same requirement is that the two parts of the unit (at the left and at the righthand side of the Feed node) can be dealt with separately, except for the presence in all the equations of both m_2 and m_3. This is not surprising, since sections 2 and 3 play a crucial role in performing the desired separation and indeed their behavior is tightly interrelated.

At this stage we have Eqs. 37 and 38, each having two solutions, so giving place to four possible combinations of solutions. The two constraints given by Eqs. 32 and 33 on the central section net flow rate ratios should then provide a criterion to decide which of the four combinations of solutions must be chosen.

To this aim let us divide Eqs. 32 and 33 by $\Omega_2^\gamma/(K_A K_D)$ and by $\Omega_1^\gamma/(K_B K_D)$ respectively, to obtain:

$$\Omega_1^\gamma < \frac{K_A K_D m_2}{\Omega_2^\gamma} < \Omega_2^\gamma \tag{45}$$

$$\Omega_1^\gamma < \frac{K_B K_D m_3}{\Omega_1^\gamma} < \Omega_2^\beta. \tag{46}$$

Using Eqs. 43 and 44, it is possible to see that the middle term in each of the inequalities above is the other root of Eqs. 37 and 38. This is a rather useful observation, since it allows us to readily identify the correct solutions of Eqs. 37 and 38 among the four possible combinations mentioned above. In particular, these are given by $\Omega_1^\gamma = \Omega_1^\ominus$ and $\Omega_2^\gamma = \Omega_2^\oplus$, so that the inequalities in Eqs. 45 and 46 reduce as follows:

$$\Omega_1^\ominus < \Omega_2^\ominus < \Omega_2^\oplus \tag{47}$$

$$\Omega_1^\ominus < \Omega_1^\oplus < \Omega_2^\beta \tag{48}$$

Thus the second inequality in Eq. 47 and the first inequality in Eq. 48 are trivially fulfilled, whereas any other choice had been made it would have taken to a contradiction.

Having determined the solution of Eqs. 37 and 38, we can proceed to determine the remaining unknowns Ω_1^α and Ω_2^β. Thus, substituting Eqs. 18 and 43 in Eq. 29 and Eqs. 17 and 44 in Eq. 30, while recalling the relationships in Eqs. 12 and 31, it is obtained:

$$\frac{K_B}{\Omega_1^\alpha} - 1 = \frac{(K_B - \Omega_1^\ominus)}{\Omega_2^\ominus}\left(1 + \frac{\epsilon_p}{\sigma(1-\epsilon_p)}\frac{\Omega_2^\ominus}{m_2\Omega_1^\ominus}\right)\frac{m_2}{m_2 + \dfrac{\epsilon_p}{\sigma(1-\epsilon_p)}}, \tag{49}$$

$$\frac{K_A}{\Omega_2^\beta} - 1 = \frac{(K_A - \Omega_2^\oplus)}{\Omega_1^\oplus}\left(1 + \frac{\epsilon_p}{\sigma(1-\epsilon_p)}\frac{\Omega_1^\oplus}{m_3\Omega_2^\oplus}\right)\frac{m_3}{m_3 + \dfrac{\epsilon_p}{\sigma(1-\epsilon_p)}}. \tag{50}$$

It is noteworthy that all the Ω values appearing in the constraint equations, 32 and 33, that is, Ω_1^γ, Ω_2^γ and Ω_2^β, depend only on the flow rate ratios m_2 and m_3. This proves that, as anticipated above, the region in the $m_2 - m_3$ plane whose points represent operating conditions which guarantee complete separation does not depend upon the values of the net flow rate ratios m_1 and m_4.

We are now in the position of further elaborating the inequalities in Eqs. 47 and 48. In particular, by substituting Eq. 50 in Eq. 48, it can be shown that the second inequality $\Omega_1^\oplus < \Omega_2^\beta$ is equivalent to the following quadratic inequality in the variable $\Omega_2^\oplus$:

$$m_3(\Omega_2^\oplus)^2 + \Omega_2^\oplus\left(\frac{\epsilon_p K_A}{\sigma(1-\epsilon_p)} - m_3\Omega_1^\oplus\right) - \frac{\epsilon_p K_A}{\sigma(1-\epsilon_p)}\Omega_1^\oplus > 0. \tag{51}$$

The lefthand side of the inequality in Eq. 51 represents a convex parabola with one positive ($\Omega_2^\oplus = \Omega_1^\oplus$) and one negative $\{\Omega_2^\oplus = -\epsilon_p K_A/[\sigma(1-\epsilon_p)m_3]\}$ root. Accordingly, the inequality in Eq. 51 is equivalent to $\Omega_1^\oplus < \Omega_2^\oplus$, and then the inequalities in Eqs. 47 and 48 reduce to the following final form:

$$\Omega_1^\ominus < \Omega_2^\ominus \tag{52}$$

$$\Omega_1^\oplus < \Omega_2^\oplus, \tag{53}$$

where all the Ω values are function only of m_2 and m_3. Since the second inequality in Eq. 47 and the first one in Eq. 48 are fulfilled by definition once the proper choice of the roots of Eqs. 37 and 38 has been done, they have been omitted in reducing inequalities in Eqs. 47 and 48 to the final expressions in Eqs. 52 and 53.

Let us make some remarks:

- Equations 52 and 53 are another way of writing the constraints on the design parameters m_2 and m_3 given by Equilibrium Theory and reported in Table 1. These equations contain only these two parameters, hence they implicitly define a region of the $m_2 - m_3$ plane where complete separation is guaranteed. The constraints on the other two design parameters are explicit and they are given in Table 1:

$$\frac{K_A}{K_D} < m_1 < +\infty \tag{54}$$

$$\frac{-\epsilon_p}{\sigma(1-\epsilon_p)} < m_4 < \frac{K_B}{K_D}. \tag{55}$$

- Optimal separation conditions are achieved when the m values are selected so as to maximize the feed flow rate ratio $1/\mu_F$ and to minimize the fresh Desorbent flow rate ratio $1/\mu_D$ (cf. Storti et al., 1989). Recalling Eqs. 34, and the corresponding relationship $1/\mu_D = \sigma(1-\epsilon_p)(m_1 - m_4)$ coming from Eqs. 19 and 31, it is readily seen that these conditions are fulfilled when m_1 and m_2 are minimum and m_3 and m_4 are maximum. For the flow rate ratios m_1 and m_4 this condition can be made explicit by using Eqs. 54 and 55 as follows:

$$m_1 = \frac{K_A}{K_D} \tag{56}$$

$$m_4 = \frac{K_B}{K_D}. \tag{57}$$

The optimal values of the flow rate ratios m_2 and m_3 are derived from Eqs. 52 and 53, following the arguments reported in detail in Appendix D, which lead to:

$$m_2 = \frac{\Omega_F}{K_A} \tag{58}$$

$$m_3 = \frac{\Omega_F}{K_B}. \tag{59}$$

The Region of Complete Separation in the $m_2 - m_3$ Plane

The conditions we have obtained in the previous section will now be used to determine the region in the $m_2 - m_3$ plane representing operating conditions which ensure complete separation. The final conditions for complete separation are given by the inequalities in Eqs. 52 and 53 which involve the roots of the quadratic Eqs. 37 and 38. Accordingly, these can be formulated in terms of equilibrium constants, feed composition and m_2 and m_3 as follows:

$$b_2 - \sqrt{b_2^2 - 4c_2} > b_1 - \sqrt{b_1^2 - 4c_1} \tag{60}$$

$$b_2 + \sqrt{b_2^2 - 4c_2} > b_1 + \sqrt{b_1^2 - 4c_1} \tag{61}$$

$$b_2^2 - 4c_2 > 0 \tag{62}$$

$$b_1^2 - 4c_1 > 0 \tag{63}$$

$$m_3 > m_2. \tag{64}$$

where the coefficients of the quadratic equations defined by Eqs. 39 to 42 have been used.

It should be noted that in order to fully characterize the region of complete separation in the $m_2 - m_3$ plane, besides the inequalities in Eqs. 60 and 61 which derive directly from Eqs. 52 and 53, three other conditions have been considered. In particular, Eqs. 62 and 63 follow from the observation that, by definition, the Ω values can take only real values. On the other hand, Eq. 64 derives from the first of Eqs. 34 by noticing that the feed flow rate μ_F must be positive. Finally, it is noteworthy that we need not impose explicitly the condition that b_2 be positive, which we have mentioned in the sixth section. In fact a necessary condition for inequalities in Eqs. 60 and 61 to be fulfilled is that b_2 is greater than b_1, which is positive for any choice of m_2 and m_3 (cf. Eq. 39). It follows that the condition $b_2 > 0$ is implied by the two inequalities in Eqs. 60 and 61.

This system of inequalities is defined in the first quadrant of the $m_2 - m_3$ plane, where it determines the region of complete separation shown in Figures 8 and 9 in the cases when $\Omega_F < K_D$ and $\Omega_F > K_D$, respectively (see Eq. 14 for the definition of Ω_F). The boundary of this region is the union of five curves, each corresponding to a portion of the curves defined by the five equations obtained by replacing in Eqs. 60 to 64 the operator $<$ with the operator $=$.

To identify the separation region quantitatively, we need to derive explicit expressions for its boundaries. This requires some further elaboration which we discuss in Appendix D, while we report in the following only the final results of the analysis. With reference to Figures 8 and 9, the following expressions for each of the five curves constituting the boundary of the complete separation region have been obtained.

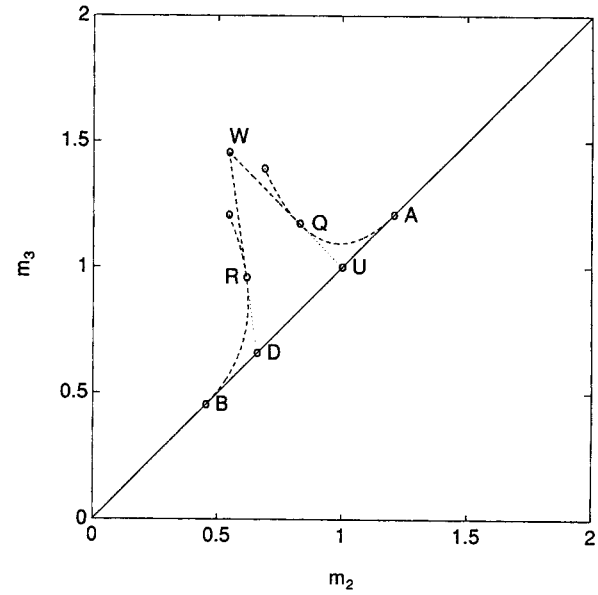

Figure 8. Region of complete separation in the $m_2 - m_3$ plane, in the case where $\Omega_F < K_D$. $K_A = 2.67$, $K_B = 1$, $K_D = 2.21$, $y_A^F = 0.5$, $y_B^F = 0.5$, $\Omega_F = 1.46$.

- Straight line WD (WR and WT) from Eqs. 60 or 61:

$$K_A(K_D - K_B)m_2 + K_B(K_A - K_D)m_3 = \Omega_F(K_A - K_B) \tag{65}$$

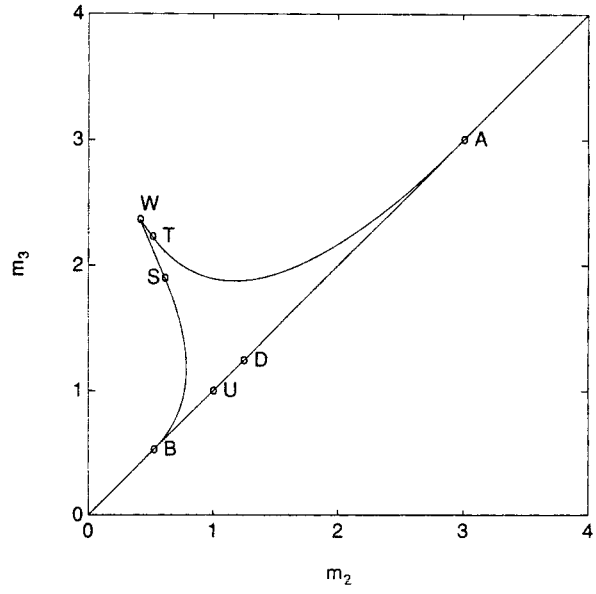

Figure 9. Region of complete separation in the $m_2 - m_3$ plane, in the case where $\Omega_F > K_D$.

$K_A = 5.71$, $K_B = 1$, $K_D = 1.9$, $y_A^F = 0.3$, $y_B^F = 0.7$, $\Omega_F = 2.37$.

- Straight line WU (WQ and WS) from Eqs. 60 or 61:

$$y_B^F m_2 + y_A^F m_3 = 1 \tag{66}$$

- Curves QA and TA from Eq. 62:

$$m_3 = m_2 + \frac{(\sqrt{K_A} - \sqrt{K_D m_2})^2}{y_A^F (K_A - K_D)} \tag{67}$$

- Curves RB and SB from Eq. 63:

$$m_2 = m_3 - \frac{(\sqrt{K_B} - \sqrt{K_D m_3})^2}{y_B^F (K_D - K_B)} \tag{68}$$

- Straight line AB from Eq. 64:

$$m_3 = m_2 \tag{69}$$

The coordinates of the points where the curve and the straight line are tangent (that is, Q and R or S and T), depend on the relative magnitude of Ω_F and K_D. On the other hand, the coordinates of all the other intersection points A, B, D, U and W in the figures are the same in both cases. The coordinates of each point are given in explicit form as follows:

point A $$\left(\frac{K_A}{K_D}, \frac{K_A}{K_D}\right) \tag{70}$$

point B $$\left(\frac{K_B}{K_D}, \frac{K_B}{K_D}\right) \tag{71}$$

point D $$\left(\frac{\Omega_F}{K_D}, \frac{\Omega_F}{K_D}\right) \tag{72}$$

point W $$\left(\frac{\Omega_F}{K_A}, \frac{\Omega_F}{K_B}\right) \tag{73}$$

point U $(1, 1)$ (74)

point Q $$\left(\frac{K_D}{K_A}, \frac{\Omega_F(K_A - K_B) - K_D(\Omega_F - K_B)}{K_B(K_A - \Omega_F)}\right) \tag{75}$$

point R $$\left(\frac{\Omega_F[K_D(K_A - K_B) - \Omega_F(K_A - K_D)]}{K_A K_D(K_D - K_B)}, \frac{\Omega_F^2}{K_B K_D}\right) \tag{76}$$

point S $$\left(\frac{\Omega_F(K_A - K_B) - K_D(K_A - \Omega_F)}{K_A(\Omega_F - K_B)}, \frac{K_D}{K_B}\right) \tag{77}$$

point T $$\left(\frac{\Omega_F^2}{K_A K_D}, \frac{\Omega_F[K_D(K_A - K_B) - \Omega_F(K_D - K_B)]}{K_B K_D(K_A - K_D)}\right) \tag{78}$$

For any given separation problem the expressions reported above allow one to readily draw the region in the $m_2 - m_3$ plane whose points correspond to complete separation operating conditions, provided that the values of m_1 and m_4 are selected in the range given by Eqs. 54 and 55. For these values of the flow rate ratios the scheme of Figure 6 and the system of Eqs. 19 to 30 are indeed correct. Hence, the solution obtained in the following section is valid and can be used to characterize the composition of each stream in the unit.

For values of m_2 and m_3 corresponding to points outside the separation region, the assumptions on which the system of Eqs. 19 to 30 is based are violated. Thus, complete separation cannot be achieved and the behavior of the unit cannot be determined using the system above. In this case, the original system of Eqs. 1 and 2 has to be solved, as discussed by Storti et al. (1989). For all operating conditions corresponding to points outside the complete separation region, this procedure allows to evaluate the composition of every stream leaving the unit, and then the relevant performance parameters.

However, for the cases mentioned above, Eqs. 19 to 30 and then the relative position of the point representing the actual unit operating conditions and the complete separation region can be used to provide at least *qualitative* information about the separation performance. These are of interest for several situations of relevance in practice, such as the case where high purity is required for only one of the two components. To this aim we will analyze more closely the physical meaning of conditions in Eqs. 60 to 63 (Eq. 64 is not examined since it represents the requirement that the feed stream flow rate should be positive).

Let us consider the condition in Eq. 60, which is shown in Appendix D to yield the boundary given by Eq. 65 when $\Omega_F < K_D$ (segment WR in Figure 8) and the boundary given by Eq. 66 when $\Omega_F > K_D$ (segment WS in Figure 9). The inequality in Eq. 60 is equivalent to the condition in Eq. 52, which in turn is a consequence of the left inequality in Eq. 45. As discussed in Appendix C, if this constraint were not fulfilled (that is, if $m_2 < \Omega_1^\gamma \Omega_2^\gamma / (K_A K_D)$), then the incoming solid state, with superscript γ in Figure 6, would prevail inside section 2. As a consequence, component B would be carried toward the Extract outlet, thus violating the requirement of complete separation for that stream.

Moreover, the condition in Eq. 63 yields the boundary given by Eq. 68, representing the curve RB in Figure 8 and the curve SB in Figure 9, which are adjacent to the segments WR and WS, respectively. The condition in Eq. 63, in its form in Eq. 68, gives an explicit lower bound on m_2, as a function of m_3. Hence, if it were violated, m_2 would be too small to desorb all component B from section 2. Thus summarizing, it can be concluded that a region to the left of line WB in Figures 8 and 9, for which either condition in Eq. 60 or the condition in Eq. 63 is violated, represents operating conditions where the Raffinate stream is pure, but the Extract stream is not.

A similar analysis can be performed on the conditions in Eqs. 61 and 62, leading to the conclusion that the region above line WA in Figures 8 and 9 represents operating conditions where the Extract stream is pure, but the Raffinate stream is not. For points far away from the complete separation region in the $m_2 - m_3$ plane no conclusions can be drawn from the analysis described above. An application of this analysis, through a comparison with experimental data, is reported in the experimental results section.

Design of Robust Countercurrent Adsorption Separation Units

We have previously determined through Eqs. 58 and 59 the optimal values of the design parameters m_2 and m_3 which maximize the feed flow rate while minimizing the fresh desorbent flow rate. It has been noted (for example, Storti et al., 1989) that in practice these optimal operating conditions are not robust, in the sense that in these conditions the unit performance is rather sensitive to small disturbances in the inlet flow rates and compositions as well as in other operating conditions. We are now in the position of fully understanding this behavior by considering that the point representing the optimal conditions, that is, point W in Figures 8 and 9 lies exactly on the boundary of the region of complete separation. It is evident that the slightest disturbance in the feed flow rates or composition as well as in the equilibrium characteristics of the system, for example, due to the aging of the desorbent, modifies the location of the point W. Such a disturbance may thus lead the operating conditions from the optimal point to a point outside the separation region.

Robustness to disturbances means that a small perturbation in the operating conditions does not modify the qualitative behavior of the unit. In other words, the unit still achieves complete separation, even though the actual performance changes, due to the mentioned disturbance. Robustness is of paramount importance in designing the operating conditions of an industrial plant, whereas sensitive operating conditions are avoided as much as possible in industrial practice.

An interesting feature of the diagrams in the $m_2 - m_3$ plane shown in Figures 8 and 9 can be evidenced by considering the first of Eqs. 34. In particular it can be seen that straight lines with unitary slope in the $m_2 - m_3$ plane correspond to operating conditions characterized by a constant value of the Feed to solid flow rate ratio, $1/\mu_F$, that is, operating conditions with the same productivity performance. Some of these straight lines, which we may refer to as isoproductivity lines, passing through the separation region are shown in Figure 10. The straight line going through the optimal point W corresponds to the highest productivity, that is, μ_F is minimum. Coming down we find straight lines corresponding to lower and lower productivities, down to the last one, $m_3 = m_2$, which is characterized by zero productivity, that is, $\mu_F = \infty$. A quantitative estimate of the robustness of a given set of operating conditions is obtained as the distance between the point representing the operating conditions and the boundary of the separation region. By looking at Figure 10 it is evident that robustness and performance vary in opposite directions. If the operating point is moved towards the optimal point W, productivity increases but robustness decreases. On the contrary, robustness can be increased by moving away from the optimal point and by choosing operating conditions represented by points lying on lines of lower productivity.

Since robustness can only be improved at the expense of productivity, before choosing the operating conditions of the unit it is important to determine an estimate of the magnitude of the possible disturbances. Different kinds of disturbances are considered in the following.

First, we consider those disturbances which affect the value of the operating parameters m_j, while leaving the boundaries of the complete separation region unchanged (that is, the equilibrium constants and the feed composition). In this case, the

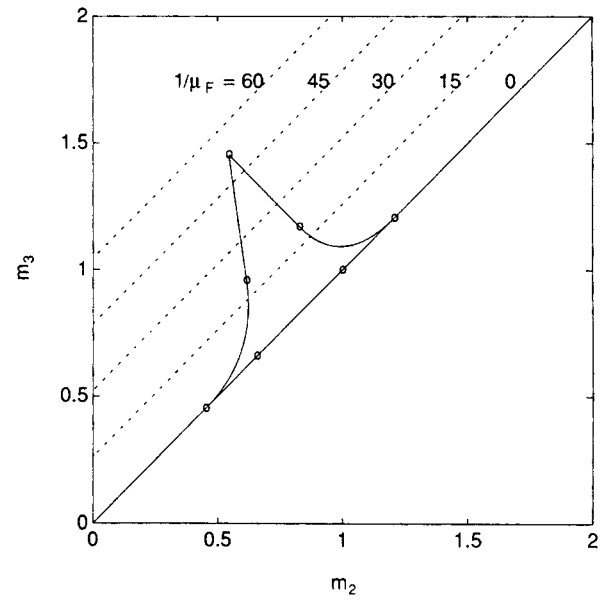

Figure 10. Region of complete separation in the $m_2 - m_3$ plane, with isoproductivity lines given by Eq. 34: $K_A = 2.67$, $K_B = 1$, $K_D = 2.21$, $y_A^F = 0.5$, $y_B^F = 0.5$, $\Omega_F = 1.46$, $\sigma = 72.6$, $\epsilon_p = 0.21$ (cf. Storti et al., 1989).

position of the representing point in the operating parameter space changes and it is the goal of robust design to guarantee that it remains within the complete separation region. Disturbances of this type include deviations in the values of the flow rates, of the operating pressure and temperature and in the loading capacity of the adsorbent solid.

The second kind of disturbances are those which affect the location of the boundaries of the complete separation region. As described in the previous section, this requires changes in the equilibrium constants or in feed composition, which in turn may be induced by adsorbent aging or feedstock variability. In both cases, the boundaries of the complete separation region move, while the location of the point representing the unit operating conditions (that is, the m_j values) remains unchanged.

In the following, both types of disturbances are considered. The aim is to provide design criteria which ensure that in the presence of these expected disturbances the point representing the unit in the operating parameter space remains inside the region of complete separation.

In general, the desired values of the net flow rate ratios are imposed indirectly through flow rate ratios controllers, either volumetric or gravimetric. Depending upon the effectiveness of the control system, deviations of various sizes from the set point value of the flow rate ratios can arise. This implies a corresponding change of the operating parameters m_j, and thus a modification of the operating regime of the unit. The effect on m_j can be evaluated by differentiating Eq. 31 as follows:

$$dm_j = \frac{1}{\sigma(1-\epsilon_p)}\, d\left(\frac{1}{\mu_j}\right) \quad \text{volumetric control}$$

$$= \frac{1}{(1-\epsilon_p)}\, d\left(\frac{1}{\mu_j \sigma}\right) \quad \text{mass control.} \tag{79}$$

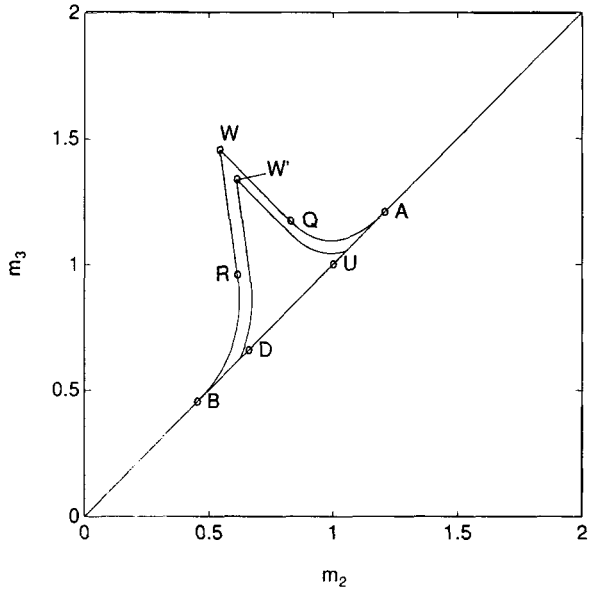

Figure 11. Region of robust complete separation in the $m_2 - m_3$ plane with respect to disturbances in the net flow rate ratios: $K_A = 2.67$, $K_B = 1$, $K_D = 2.21$, $y_A^F = 0.5$, $y_B^F = 0.5$, $\Omega_F = 1.46$, $dm = 0.02$.

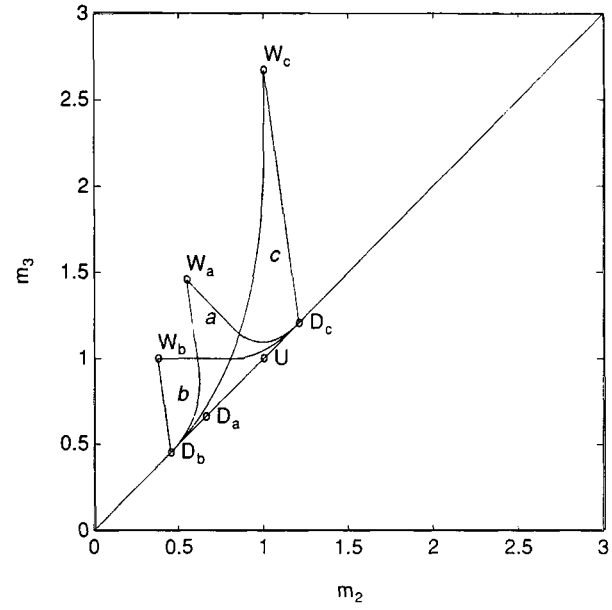

Figure 12. Effect of feed composition changes on the region of complete separation in the $m_2 - m_3$ plane: $K_A = 2.67$, $K_B = 1$, $K_D = 2.21$.

(a) $y_A^F = 0.5$, $y_B^F = 0.5$, $\Omega_F = 1.46$; (b) $y_A^F = 1$, $y_B^F = 0$, $\Omega_F = 1$; (c) $y_A^F = 0$, $y_B^F = 1$, $\Omega_F = 2.67$. The straight line $W_b - W_c$ is the locus of the optimal points.

Another source of disturbances, particularly when the unit is operated in the vapor phase, can be due to perturbations in the values of the operating pressure and temperature. The fluid density, which enters the model equations through the parameter σ, is affected by these variations and it produces a corresponding change in the operating parameters. By differentiating Eq. 31, under the assumption of perfect flow control, we can qualitatively estimate such a change:

$$dm_j = \frac{1/\mu_j - \epsilon_p}{\rho_s \Gamma^\infty (1-\epsilon_p)}\, d\rho \quad \text{volumetric control}$$

$$= \frac{-\epsilon_p}{\rho_s \Gamma^\infty (1-\epsilon_p)}\, d\rho \quad \text{mass control.} \qquad (80)$$

Following the previous analysis, or similar ones when a different type of disturbance is considered, it is possible to estimate an upper bound dm for the disturbances on m_j. This estimate can be used to draw the robust complete separation region in the $m_2 - m_3$ plane sketched in Figure 11, which is readily obtained by properly shifting the boundary of the complete separation region determined above. Every point in the newly obtained region represents robust operating conditions, whereas point W' represents the optimal productivity operating conditions within the region of robust operations.

Next we consider disturbances or uncertainties in the feed composition. These imply a correspondent variation in the parameter Ω_F and then a change of the entire separation region.

In order to better investigate such a change, we first consider the properties in Figures 8 and 9, which are invariant with the change of feed composition. These invariant properties are: the coordinates of the points A, B and U, the slope of the straight line WD and the fact that the point U belongs to the straight line WU. Therefore, as the feed composition changes, the straight line WD (cf. Eq. 65) describes a family of parallel lines, whereas the straight line WU (cf. Eq. 66) describes a family of lines passing through the point U. The curves AQ and BR in Figure 8 (or AT and BS in Figure 9) change with Ω_F but their extreme points A and B do not. Another interesting property is that the straight line WU does not depend on the equilibrium constants; in particular if the feed composition is equimolar, its equation is $m_2 + m_3 = 2$.

Thus summarizing, the change of the complete separation region as a function of the feed composition, y_A^F (or Ω_F), is shown in Figure 12. When the feed is constituted of pure component A (case b), that is, $y_A^F = 1$ (or $\Omega_F = K_B$), the line WU is horizontal and the three points B, D and R collapse together. On the other extreme, when the feed is constituted of pure component B (case c), that is, $y_A^F = 0$ (or $\Omega_F = K_A$), the line WU is vertical and the three points A, D and T coincide. While Ω_F goes from K_B to K_A the slope of this straight line changes from zero to $-\infty$. The optimal point goes from the lower left, point $(K_B/K_A, 1)$, to the upper right, point $(1, K_A/K_B)$, along the straight line of equation $K_B m_3 = K_A m_2$. At the particular feed composition where $\Omega_F = K_D$ the two lines WU and WD coincide. In this situation, which corresponds to the bifurcation point between the picture in Figure 8 and that in Figure 9, the separation region is not endowed with the degeneracy of the triangle WUD, which vanishes into a segment. For values of Ω_F not close to K_D the triangle WUD is a good approximation of the complete separation region.

If an upper and lower bound on the values that Ω_F can assume around its nominal value due to feed composition disturbances can be estimated, then three different complete separation regions can be drawn for the nominal value and for the upper

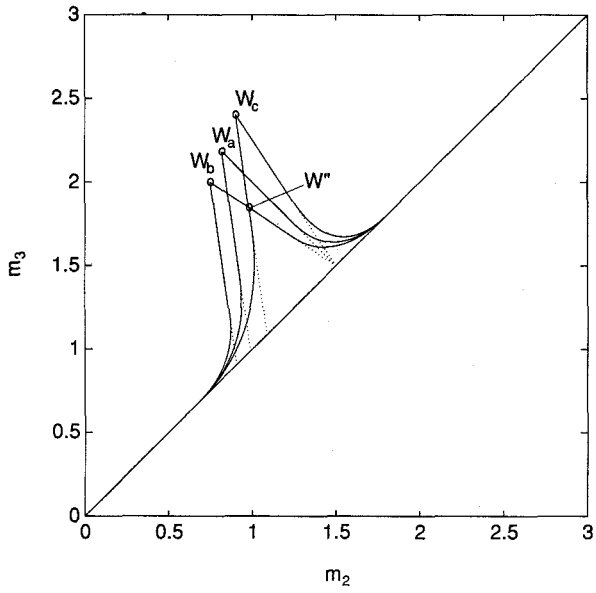

Figure 13. Region of robust complete separation in the $m_2 - m_3$ plane with respect to feed composition changes: $K_A = 2.67$, $K_B = 1$, $K_D = 2.21$.

(a) $y_A^F = 0.5$, $y_B^F = 0.5$, $\Omega_F = 1.46$; (b) $y_A^F = 0.6$, $y_B^F = 0.4$, $\Omega_F = 1.33$; (c) $y_A^F = 0.4$, $y_B^F = 0.6$, $\Omega_F = 1.60$.

and lower bounds. As shown in Figure 13, in this case the region of robust complete separation is given by the intersection of the three regions above, while the point W'' represents the optimal productivity operating conditions.

Robust operating conditions for the first and the fourth section are easily determined. Since the position of the complete separation region in the $m_1 - m_4$ plane (cf. Eqs. 54, 55) is determined only by the equilibrium ratios, only those disturbances that can affect the actual value of the net flow rate ratios m_1 and m_4 have to be considered. As mentioned above these include changes in the stream flow rates or temperature and pressure disturbances. Once a value of the upper bound dm has been estimated, robust operations are guaranteed if the operating conditions are chosen so that $m_1 \geq (K_A/K_D + dm)$ and $m_4 \leq (K_B/K_D - dm)$.

Finally, it is worth mentioning the changes in the unit performance which are induced by the changes, usually rather slow in time, of the equilibrium characteristics due to the adsorbent aging. One way to account for these changes is again a robust design of the operating conditions.

Often in applications the adsorbent aging induces a change only in the adsorbent loading capacity Γ^∞. This situation can be regarded as a disturbance of the first kind above. Accordingly, an estimate of the effect of this change on the values of the operating parameters m_j can be obtained as follows:

$$dm_j = \frac{\rho(1/\mu_j - \epsilon_p)}{\rho_s(1-\epsilon_p)}\, d\left(\frac{1}{\Gamma^\infty}\right) \quad \text{volumetric/mass control.} \qquad (81)$$

Similarly as in the case of Eqs. 79 and 80, the estimate given by Eq. 81 can be used directly to derive the robust complete separation region sketched in Figure 11.

On the other hand, if the adsorbent aging affects the selectivities of the components present in the system, then the location of the boundaries of the separation region changes, as in the case of disturbances of the second kind examined above. Accordingly, the same procedure can be followed for a robust design of the unit.

Table 2. Operating, Adsorbent and Equilibrium Parameters

Equilibrium Parameters	
Γ^∞	0.135 kg/kg
K_B	1
K_D	1.50
K_A	1.95
Operating temperature	523 K
Operating pressure	3×10^6 Pa
Feed composition	$y_A^F = 0.49$, $y_B^F = 0.51$
ϵ	0.42
ϵ_p	0.21
ρ_s	1,490 kg/m^3
ρ_f	7 kg/m^3
A	1.767×10^{-4} m^2
L	1 m

Experimental Results

As mentioned in the Introduction section, most applications of continuous countercurrent adsorption separations involve the simulated moving bed technology. Since true continuous countercurrent models can be used conveniently to simulate this kind of apparatus, it is possible to test the theoretical results obtained in this work by comparison with experimental steady-state data relative to a SMB unit. In particular, we consider the results obtained by Storti et al. (1992) in a six port SMB pilot-plant operated in the vapor phase to separate a mixture of *m*- and *p*-xylene using Isopropylbenzene as desorbent and KY zeolites as adsorbent.

To compare the experimental operating parameters of the SMB unit with the complete separation region obtained in this work with a TCC model, the kinematic similarity between the two units has been used (Ruthven and Ching, 1989; Storti et al., 1992). Since in the experimental apparatus considered the controlled variables are the mass flow rates G_j, in order to compute the flow rate ratios m_j, it is convenient to rewrite Eq. 4 in the following form:

$$m_j = \frac{G_j t^* - AL\epsilon^* \rho_f}{AL\rho_s \Gamma^\infty (1-\epsilon^*)} \quad (j = 1, \ldots, 4). \qquad (82)$$

where the solid velocity in the TCC unit, u_s, has been evaluated through the kinematic similarity relationship as follows: $u_s = (1-\epsilon)L/t^*$. The operating conditions adopted in the experimental analysis are summarized in Table 2, together with the values of the physico-chemical parameters involved in Eq. 82 and the constant ratios appearing in the equilibrium model in Eq. 8. The adsorbed phase saturation concentration Γ^∞ and the equilibrium constant ratios K_i have been estimated by fitting the results of some preliminary breakthrough experiments performed directly on the SMB pilot plant.

In Figure 14 the complete separation region for the system under examination has been drawn in the $m_2 - m_3$ plane using Eqs. 65 to 78, where the equilibrium ratios and the feed composition have been taken from Table 2, while $\Omega_F = 1.33$ from Eq. 14. On the other hand, the location of the points representing the experimental runs has been obtained by evaluating

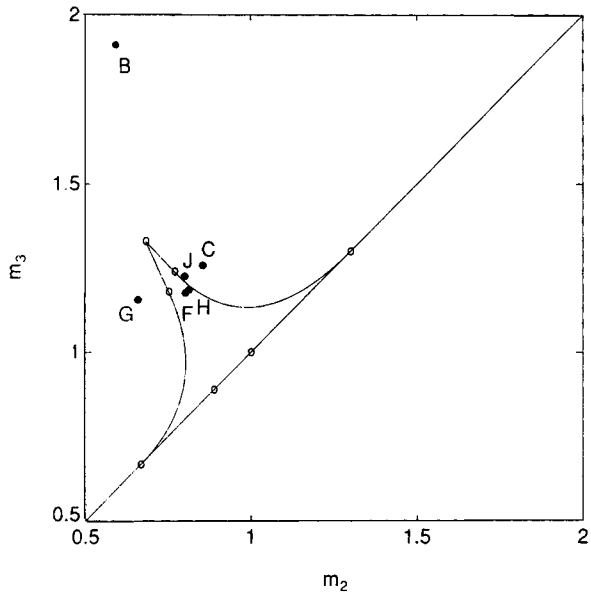

Figure 14. Comparison of the predicted region of complete separation in the $m_2 - m_3$ plane with the experimental data (•) (Storti et al., 1992): $K_A = 1.95$, $K_B = 1$, $K_D = 1.50$, $y_A^F = 0.49$, $y_B^F = 0.51$, $\Omega_F = 1.33$.

the operating parameters m_2 and m_3 from Eq. 82. The obtained values for each experimental run are summarized in Table 3. In the same table, the purity of the Raffinate stream (P_R) and the purity of the Extract stream (P_E) measured experimentally are also reported, together with the values predicted by the equilibrium theory model in Eqs. 1 to 3. It can be seen that, as expected, the quantitative agreement between experimental and calculated values is not very close, because of the approximations intrinsic in the equilibrium theory model. Nevertheless, as discussed in the following, the location of the experimental points with respect to the complete separation region is fully coherent with the observed separation performance of the unit. This assesses the reliability and utility of the results of the analysis developed in this work in determining the performance of the examined separation units.

Let us consider the relative position of the points representing the experimental runs with respect to the predicted complete separation region shown in Figure 14. The comparison between experimental and theoretical results can be performed along the lines followed in the last part of the seventh section. Thus, the experimental runs F and H, where as reported in Table 3 complete separation has been achieved, are represented by the points in the $m_2 - m_3$ plane shown in Figure 14, which lie well within the complete separation region.

A different behavior is found when considering the experimental runs C, G and J, which lie outside the complete separation region in Figure 14. In particular, in Table 3 it can be seen that in the experimental runs C and J complete separation has not been achieved in the Raffinate. This is consistent with the geometrical observation that the corresponding points in the $m_2 - m_3$ plane lie above line WA in Figure 14, that is, in a region where the presence of component A in the Raffinate is theoretically predicted, as discussed in the last part of the seventh section. It is worth noticing that the point corresponding to run J is very close to the boundary of the complete separation region. This is in good agreement with the experimental separation performance, which in Table 3 can be seen to be indeed very close to complete separation.

Table 3. Comparison of the Experimental and Calculated Separation Performances

	Flow Rate Ratio				Purity Experimental		Purity Calculated	
Run	m_1	m_2	m_3	m_4	P_E (%)	P_R (%)	P_E (%)	P_R (%)
F	3.583	0.798	1.167	0.379	>99.7	>99.9	100	100
G	3.583	0.655	1.146	0.409	89.5	>99.9	81.0	100
C	3.583	0.850	1.249	0.368	>99.6	84.6	100	84.6
B	2.858	0.589	1.900	0.434	81.0	69.0	88.2	69.2
H	2.518	0.809	1.177	0.501	>99.8	>99.9	100	100
J	2.057	0.796	1.216	0.529	>99.9	99.7	100	99.4

On the contrary, in run G complete separation was not achieved because of the presence of about 10% of *m*-Xylene in the Extract stream. As shown in Figure 14, in this case the point representing run G falls to the left of the complete separation region, that is, to the left of line WB, where as theory predicts the operating conditions are such that component B is not completely desorbed from section 2, and it is then carried toward the Extract outlet.

Finally, also the rather poor separation performance reported in Table 3 for the experimental run B compares well with the long distance separating the point representing this run from the complete separation region in Figure 14. Thus, summarizing, we can conclude that the results of the developed analysis allow us to correctly interpret the experimental performances of the SMB pilot plant reported by Storti et al. (1992). Moreover, it is remarkable how the knowledge of the location of the complete separation region makes it easy to understand the behavior of these units and to select the operating conditions required to obtain a given separation performance.

Concluding Remarks

The separation of a binary mixture in a four section countercurrent adsorption separation unit, using a third component having intermediate adsorptivity as desorbent, has been considered. The analysis is developed in the frame of equilibrium theory, where the adsorption equilibria are described through the constant selectivity stoichiometric model, while mass-transfer resistances and axial mixing are neglected. This model has been acknowledged as being capable of describing the key features of the adsorption separation processes. Accordingly, in this work it has been used to develop a procedure for the optimal and robust design of a four section separation unit, by taking advantage of the available explicit solution of the adsorption problem associated with each section of the unit.

By requiring that the unit achieves complete separation, it has been possible to identify a set of implicit constraints on the operating parameters, that is, the flow rate ratios in the four sections of the unit, from which explicit bounds on the operating parameters are obtained. This procedure yields a region in the operating parameters space, which can be drawn *a priori* in terms of the adsorption equilibrium constants and the feed composition. It has been shown that in the case of a linear equilibrium model the corresponding region is much

simpler than in the nonlinear case, where the role of the desorbent adsorptivity and the effect of the feed composition are fully taken into account.

In spite of the richness of the information which are carried by the geometric representation of the complete separation region in the $m_2 - m_3$ plane, its construction and its practical use are remarkably simple, involving only explicit algebraic relationships. In particular, it provides a very effective tool to determine both optimal and robust operating conditions. The latter requirement has been carefully analyzed by first determining the various possible sources of disturbances, as well as their effect on the separation performance. Then, a procedure has been developed to modify the complete separation region into a "robust" complete separation region, once an estimate of the possible errors in the operating parameters of the unit has been evaluated.

The reliability and accuracy of these theoretical findings have been assessed by comparison with a set of experimental results obtained in a six port Simulated Moving Bed adsorption separation unit operated in the vapor phase.

Notation

A = cross section of the adsorption column
b_1, b_2, c_1, c_2 = coefficients of the quadratic Eqs. 37 and 38 defined by Eqs. 39 to 42
f_i^j = dimensionless net flow rate of component i in section j, $f_i^j = m_j y_i^j - \theta_i^j$
G_j = fluid mass-flow rate in section j of a SMB unit
K_i = equilibrium constant of adsorption of component i
L_j = length of section j
m_j = mass-flow rate ratio in section j (cf. Eq. 4 and Eq. 82)
NC = total number of components
P_E = extract purity, $P_E = y_A^E/(y_A^E + y_B^E)$
P_R = raffinate purity, $P_R = y_B^R/(y_A^R + y_B^R)$
t = time
t^* = switching time in a SMB unit
u_j = superficial fluid phase velocity in section j
u_s = superficial solid phase velocity
x = dimensionless axial coordinate, $x = z/L_j$
y_i^j = fluid phase dimensionless concentration of component i in section j
z = axial coordinate

Greek letters

Γ^∞ = adsorbed phase saturation concentration
ϵ = external void fraction
ϵ_p = intraparticle void fraction
ϵ^* = overall void fraction, $\epsilon^* = \epsilon + \epsilon_p(1-\epsilon)$
θ_i^j = adsorbent coverage fraction of component i in section j
μ_j = volumetric flow rate ratio in section j, $\mu_j = u_s/u_j$
ρ_f = fluid phase density
ρ_s = bulk solid mass density
σ = capacity ratio, $\sigma = \rho_s \Gamma^\infty/\rho_f$
τ = dimensionless time, $\tau = tu_s/L$
Φ = equilibrium theory parameter defined by Eq. A7
Ω = equilibrium theory parameter defined by Eq. 9 or 10

Subscripts and superscripts

a = section a
A, B = components to be separated
b = section b
c = column state
D = desorbent
E = extract
f = fluid state
F = feed
i = component index
j = section index
o = initial condition
p = outgoing state, after mixing
R = raffinate
s, S = solid state
α, β, γ = streams in the four section separation unit (cf. Figure 6)
$\oplus, \ominus$ = greatest and smallest root of a quadratic equation, respectively

Literature Cited

Balannec, B., and G. Hotier, "From Batch Elution to Simulated Counter-current Chromatography," in *Preparative and Production Scale Chromatography with Applications*, G. Ganetsos and P. E. Barker, eds., Marcel Dekker, New York, in press (1992).

Broughton, D. B., and C. G. Gerhold, "Continuous Sorption Process Employing Fixed Beds of Sorbent and Moving Inlets and Outlets," U.S. Patent 2,985,589 (May 23, 1961).

Ching, C. B., and D. M. Ruthven, "An Experimental Study of a Simulated Counter-current Adsorption System: I. Isothermal Steady-State Operation," *Chem. Eng. Sci.*, **40**, 877 (1985).

Ching, C. B., D. M. Ruthven, and K. Hidajat, "Experimental Study of a Simulated Counter-current Adsorption System: III. Sorbex Operation," *Chem. Eng. Sci.*, **40**, 1411 (1985).

Hashimoto, K., S. Adachi, H., Noujima, and H. Maruyama, "Models for the Separation of Glucose/Fructose Mixture Using a Simulated Moving-Bed Adsorber," *J. Chem. Eng. Japan*, **16**, 400 (1983).

Johnson, J., "SORBEX: Continuing Innovation in Liquid Phase Adsorption," in *NATO ASI Adsorption: Science and Technology*, A. E. Rodrigues et al., eds., Kluwer Academic Publishers (1989).

Rhee, H.-K., R. Aris, and N. Amundson, "Multicomponent Adsorption in Continuous Countercurrent Exchangers," *Phil. Trans. Roy. Soc. London*, **A269**, 187 (1971).

Rhee, H.-K., R. Aris, and N. Amundson, *First-Order Partial Differential Equations*, Vol. II, Prentice-Hall Inc., Englewood Cliffs, NJ (1989).

Ruthven, D. M., *Principles of Adsorption and Adsorption Processes*, Wiley, New York (1984).

Ruthven, D. M., and C. B. Ching, "Counter-Current and Simulated Counter-Current Adsorption Separation Processes," *Chem. Eng. Sci.*, **44**, 1011 (1989).

Storti, G., M. Masi, S. Carrà, and M. Morbidelli, "Optimal Design of Multicomponent Adsorption Separation Processes Involving Nonlinear Equilibria," *Chem. Eng. Sci.*, **44**, 1329 (1989).

Storti, G., M. Mazzotti, L. T. Furlan, M. Morbidelli, and S. Carrà, "Performance of a Six Port Simulated Moving Bed Adsorption Pilot Plant for Vapor-Phase Separations," *Sep. Sci. & Technol.*, **27**, 1889 (1992).

Appendix A

Before proving theorem 1 it is necessary to recall the main results from equilibrium theory applied to stoichiometric systems with NC components (Storti et al., 1989).

Through equilibrium theory it is demonstrated that there is a one-to-one mapping between the space of fluid or adsorbed phase concentrations and a (NC − one)-dimensional space, whose components are obtained as roots of the equation:

$$\sum_{i=1}^{NC} \frac{K_i y_i}{K_i - \Omega} = 0, \qquad \text{(A1)}$$

or

$$\sum_{i=1}^{NC} \frac{\theta_i}{K_i - \Omega} = 0. \quad \text{(A2)}$$

Moreover, the Ω parameters are roots of the equation:

$$\sum_{i=1}^{NC} \frac{K_i \theta_i}{K_i - \Omega} = 1, \quad \text{(A3)}$$

and fulfill the following inequalities:

$$K_1 \le \Omega_1 \le K_2 \le \ldots \le K_i \le \Omega_i \le K_{i+1} \le \ldots \le K_{NC-1} \le \Omega_{NC-1} \le K_{NC}, \quad \text{(A4)}$$

where $\Omega = K_i$ if and only if $y_i = \theta_i = 0$. Equations A1 and A2 can be inverted leading for $i = 1, \ldots, NC$ to:

$$\theta_i = \left(\prod_{j=1}^{NC-1} (K_i - \Omega_j) \right) \Big/ \left(\prod_{j=1,\, j \ne i}^{NC} (K_i - K_j) \right), \quad \text{(A5)}$$

$$y_i = \theta_i \left(\prod_{j=1,\, j \ne i}^{NC} K_j \right) \Big/ \left(\prod_{j=1}^{NC-1} \Omega_j \right). \quad \text{(A6)}$$

Let us now consider the single section in Figure 3, and the two incoming states corresponding to the vectors Ω^a and Ω^b. Let Φ_k be:

$$\Phi_k = \left(\prod_{j=1}^{k-1} \Omega_j^a \right) \left(\prod_{j=k+1}^{NC-1} \Omega_j^b \right) \Big/ \left(\prod_{j=1}^{NC} K_j \right) \quad (k = 1, \ldots, NC-1). \quad \text{(A7)}$$

At steady-state conditions the fluid and adsorbed phases have the same composition in the entire column. The particular composition is determined by the value of the net flow rate ratio m and the corresponding Ω^c vector can take one of the following general configurations:

- The state inside the column is characterized by the vector:

$$\Omega^c = (\Omega_1^a, \ldots, \Omega_k^a, \Omega_{k+1}^b, \ldots, \Omega_{NC-1}^b), \quad k = 0, \ldots, NC-1, \quad \text{(A8)}$$

where k can take any of the integer values between 0 and $NC-1$, depending upon which one of the following intervals contains the value of the net flow rate ratio, m:

$$\frac{-\epsilon_p}{\sigma(1-\epsilon_p)} \le m \le \Phi_1 \Omega_1^b \min\{\Omega_1^a, \Omega_1^b\}, \quad k = 0, \quad \text{(A9)}$$

$$\Phi_k \Omega_k^a \max\{\Omega_k^a, \Omega_k^b\} \le m \le \Phi_{k+1} \Omega_{k+1}^b \min\{\Omega_{k+1}^a, \Omega_{k+1}^b\}, \quad k = 1, \ldots, NC-2, \quad \text{(A10)}$$

$$\Phi_{NC-1} \Omega_{NC-1}^a \max\{\Omega_{NC-1}^a, \Omega_{NC-1}^b\} \le m < +\infty, \quad k = NC-1. \quad \text{(A11)}$$

- In the case where $\Omega_k^b < \Omega_k^a$ for some $k = 1, \ldots, NC-1$, then the constant state can correspond to the vector:

$$\Omega^c = (\Omega_1^a, \ldots, \Omega_{k-1}^a, \Omega_k, \Omega_{k+1}^b, \ldots, \Omega_{NC-1}^b), \quad \text{(A12)}$$

with $\Omega_k^b < \Omega_k < \Omega_k^a$ and $m = \Phi_k \Omega_k^2$.

By identifying the fluid stream with the superscript f, the solid stream with s and the constant state inside the column with c, the single component material balance at either end of the column can be written as:

$$y_i^f = \mu(1-\epsilon_p)\sigma \left[(m y_i^c - \theta_i^c) + \left(\frac{\epsilon_p}{(1-\epsilon_p)\sigma} y_i^s + \theta_i^s \right) \right]. \quad \text{(A13)}$$

Let $F(\Omega)$, $C(\Omega)$ and $S(\Omega)$ be the functions whose zeroes are the Ω values characterizing the fluid, constant and solid states respectively:

$$F(\Omega) = \sum_{i=1}^{NC} \frac{K_i y_i^f}{K_i - \Omega}, \quad \text{(A14)}$$

$$C(\Omega) = \sum_{i=1}^{NC} \frac{\theta_i^c}{K_i - \Omega}, \quad \text{(A15)}$$

$$S(\Omega) = \sum_{i=1}^{NC} \frac{K_i y_i^s}{K_i - \Omega}. \quad \text{(A16)}$$

All these functions have strictly positive first derivatives. If we multiply Eq. A13 by $K_i/(K_i - \Omega)$, the sum over the index i and use the equilibrium model Eq. 8 and the inverse relationship in Eq. A6, after some algebraic manipulations we obtain the equation:

$$\frac{F(\Omega)}{\mu(1-\epsilon_p)\sigma} = \left(m \frac{\Pi_{j=1}^{NC} K_j}{\Pi_{j=1}^{NC-1} \Omega_j^c} - \Omega \right) C(\Omega) + \left(\frac{\Omega}{\Sigma_{j=1}^{NC} K_j y_j^s} + \frac{\epsilon_p}{(1-\epsilon_p)\sigma} \right) S(\Omega), \quad \text{(A17)}$$

which involves the three functions $F(\Omega)$, $C(\Omega)$ and $S(\Omega)$ defined above.

Let us consider the second part of theorem 1, and let us assume that the constant state inside the column and the incoming solid (or fluid) stream share the same Ω value, say Ω^*. Therefore, $C(\Omega^*)$ and $S(\Omega^*)$ [or $F(\Omega^*)$] are equal to zero. From Eq. A17 it follows that also $F(\Omega^*) = 0$ [or $S(\Omega^*) = 0$], hence Ω^* is one of the Ω values which characterize the outgoing fluid (or solid) stream. This proves the second part of theorem 1.

Now, consider the first part of theorem 1. Let $\overline{\Omega}_k = \max\{\Omega_k^a, \Omega_k^b\}$ and $\underline{\Omega}_k = \min\{\Omega_k^a, \Omega_k^b\}$. Using Eqs. A7, A8 and A12, Eq. A17 reduces to:

$$\frac{F(\Omega)}{\mu(1-\epsilon_p)\sigma} = \left(\frac{m}{\Phi_k \Omega_k^c} - \Omega \right) C(\Omega) + \left(\frac{\Omega}{\Sigma_{j=1}^{NC} K_j y_j^s} + \frac{\epsilon_p}{(1-\epsilon_p)\sigma} \right) S(\Omega). \quad \text{(A18)}$$

We now proceed with the proof by considering first the right end of the column. In this case we should assume that in Eq. A18 the incoming adsorbed state (that is, Ω^b) is known, while the outgoing fluid state (that is, Ω^f) has to be determined. As mentioned above, two cases may arise depending on the configuration of the constant state inside the column.

Case 1. Ω^c given by Eq. A8. For $k=0$ the adsorbed state prevails within the column (that is, $\Omega^c=\Omega^b$) and the property proven above implies that the outgoing fluid stream has the same Ω vector as the incoming solid stream (that is, $\Omega^f=\Omega^b$). For $k=1, \ldots, NC-1$, the lower bound constraint of Eq. A10, together with Eq. A18, implies:

$$\frac{F(\Omega)}{\mu(1-\epsilon_p)\sigma} \geq (\bar{\Omega}_k-\Omega)C(\Omega) + \left(\frac{\Omega}{\Sigma_{j=1}^{NC}K_j y_j^b}+\frac{\epsilon_p}{(1-\epsilon_p)\sigma}\right)S(\Omega). \quad \text{(A19)}$$

If $i \geq k+1$ then $\Omega_i^c=\Omega_i^b$, hence the statement proven above can be applied, yielding $\Omega_i^f=\Omega_i^b$.

Some further considerations are needed for the remaining elements of the fluid state Ω vector, that is, Ω_i^f with $i \leq k$. From Eq. A4 it is readily seen that $(\bar{\Omega}_k-\bar{\Omega}_i) \geq 0$ and $(\bar{\Omega}_k-\underline{\Omega}_i) \geq 0$. On the other hand, recalling that for each $i=1, \ldots, k$, both $\bar{\Omega}_i$ and $\underline{\Omega}_i$ belong to the interval $[K_i, K_{i+1}]$, and that $C(\Omega)$ and $S(\Omega)$ are strictly increasing functions within the same interval with $C(\Omega_i^a)=0$ and $S(\Omega_i^b)=0$, it follows that $C(\bar{\Omega}_i) \geq 0$, $S(\bar{\Omega}_i) \geq 0$, $C(\underline{\Omega}_i) \leq 0$ and $S(\underline{\Omega}_i) \leq 0$. When substituted in Eq. A19, these results lead to the conclusion that $F(\bar{\Omega}_i) \geq 0$ and $F(\underline{\Omega}_i) \leq 0$, implying, through similar reasoning, that the i-th element of the fluid state vector where $F(\Omega_i^f)=0$ is bounded as follows:

$$\underline{\Omega}_i \leq \Omega_i^f \leq \bar{\Omega}_i \quad (i=1, \ldots, NC-1). \quad \text{(A20)}$$

The results obtained above for $i \geq k+1$ have also been included in the last equation.

Case 2. Ω^c given by Eq. A12. Since in this case $m=\Phi_k\Omega_k^2$, Eq. A18 reduces to:

$$\frac{F(\Omega)}{\mu(1-\epsilon_p)\sigma} = (\Omega_k-\Omega)C(\Omega) + \left(\frac{\Omega}{\Sigma_{j=1}^{NC}K_j y_j^b}+\frac{\epsilon_p}{(1-\epsilon_p)\sigma}\right)S(\Omega), \quad \text{(A21)}$$

where $k=1, \ldots, NC-1$. For $i<k$ and $i>k$ the same arguments as in the previous case can be repeated leading again to the condition in Eq. A20. On the other hand, for $i=k$, since $S(\Omega_k)>0$, Eq. A21 implies that $F(\Omega_k)>0$. Similarly, from Eq. A21 since $(\Omega_k-\Omega_k^b)C(\Omega_k^b)<0$ and $S(\Omega_k^b)=0$, hence $F(\Omega_k^b)<0$. It follows that $\Omega_k^b<\Omega_k^f<\Omega_k<\Omega_k^a$.

We have then proved the first part of theorem 1 with reference to the fluid state leaving the column from the right end in Figure 3.

The same proof should be repeated with reference to the adsorbed state leaving the left end of the column. However, since it proceeds through arguments which are fully symmetric to those followed in the previous case, we omit its derivation.

Appendix B

Theorem 1 establishes that the Ω vectors characterizing the constant state inside the column and the two outgoing streams are bounded by the Ω vectors of the two incoming streams.

In the following, we prove that an analogous constraint exists when considering the mixing process of two streams at a node of a separation unit (cf. Figure 6). In particular, the Ω vector characterizing the outgoing stream is constrained by the Ω vectors of the two incoming streams.

The single component material balances at a node can be written as follows:

$$y_i^p = \alpha y_i^a + (1-\alpha)y_i^b, \quad \text{(B1)}$$

where a and b are the two incoming fluid streams, p is the outgoing stream and $0 \leq \alpha \leq 1$. The Ω values of the outgoing stream are the zeroes of the function:

$$Z(\Omega) = \sum_{i=1}^{NC}\frac{K_i y_i^p}{K_i-\Omega} = \alpha\sum_{i=1}^{NC}\frac{K_i y_i^a}{K_i-\Omega} + (1-\alpha)\sum_{i=1}^{NC}\frac{K_i y_i^b}{K_i-\Omega}, \quad \text{(B2)}$$

whereas the two sums in the righthand side define two functions whose zeroes are the elements of the two vectors Ω^a and Ω^b characterizing the two incoming streams. Since both the functions, as well as $Z(\Omega)$, are strictly increasing with Ω in the interval $[K_i, K_{i+1}]$ to which the values Ω_i^a, Ω_i^b and Ω_i^p belong, it can be concluded that for each $i=1, \ldots, NC-1$:

$$Z(\min\{\Omega_i^a, \Omega_i^b\}) \leq 0 \leq Z(\max\{\Omega_i^a, \Omega_i^b\}) \quad (i=1, \ldots, NC-1), \quad \text{(B3)}$$

and then

$$\min\{\Omega_i^a, \Omega_i^b\} \leq \Omega_i^p \leq \max\{\Omega_i^a, \Omega_i^b\} \quad (i=1, \ldots, NC-1). \quad \text{(B4)}$$

Let us now consider the four section unit shown in Figure 6. We can see that with the only exception of the two incoming streams (that is, Feed and Desorbent), each stream in the unit may be regarded as derived from the others in one of the two following ways. The constant state inside each column as well as all the outgoing streams can be determined from the composition of the incoming streams, using the solution of the single section problem outlined above. Similarly, the streams leaving the mixing nodes (at the feed and desorbent inlets) are determined by the two inlet streams. In both cases, using theorem 1 and Eq. B4 respectively, we know that the obtained Ω vectors are bounded by those of the incoming streams. Since this applies to all streams in the unit except the Feed and Desorbent, by recursively using this result, we can derive the condition in Eq. 15, thus completing the proof of theorem 2.

Appendix C

The purpose of Appendix C is to prove the complete separation proposition which is stated in theorem 3. For each section of the four section unit, theorem 3 determines the steady constant state which is compatible with the requirement of complete separation under robust operation. The Ω values characterizing these states and the corresponding constraints

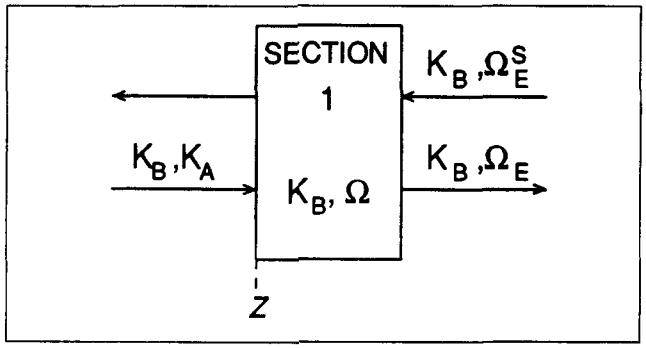

Figure 15. Section 1, when the constant state prevailing inside the column is different from the fluid state.

on the net flow rate ratios are reported in Table 1. The proof of the theorem requires that for each section of the unit all the possible constant states derived from the scheme in Figure 6 are determined and that their consistence with the requirement of complete separation under robust operation is discussed. We will see that for each section only one configuration is consistent with all the others. The possible constant states and the corresponding net flow rate ratio ranges are determined according to the results summarized by Storti et al., 1989, and reported in the general case of a *NC*-component system in Appendix A.

It is worth remembering here that the operating conditions to obtain complete separation must fulfill the requirements of complete separation illustrated in the scheme of Figure 6. The points corresponding to these admittable operating conditions constitute a set in the space of the operating parameters m_1, m_2, m_3 and m_4. The additional requirement of robustness imposes that the operating conditions are not sensitive to small perturbations. It follows that from a mathematical point of view the robust operating conditions are only those, corresponding to the internal points of the set mentioned above, that is, points for which a neighborhood entirely contained in the set does exist.

Sections 1 and 4

Let us start by considering section 1. There is only one transition between the solid state (K_B, Ω_E^S) and the fluid state (K_B, K_A). It is a simple wave since $\Omega_E^S \leq K_A$. The only admittable steady constant state is the fluid state, which prevails inside the column provided that $m_1 \geq K_A/K_D$. In fact if it were not like this, the constant state inside the column would be characterized by the pair (K_B, Ω), where $\Omega_E^S \leq \Omega < K_A$ (the solid state prevails when $\Omega = \Omega_E^S$, whereas a state across the simple wave prevails in all the other cases). The material balance of component A at boundary Z in Figure 15 would read:

$$y_A^1\left(\frac{\Omega}{K_D} - m_1\right) = \theta_A^s + \frac{\epsilon_p}{(1-\epsilon_p)\sigma} y_A^s, \qquad \text{(C1)}$$

and y_A^s, and hence θ_A^s, should be equal to zero for complete separation to be obtained. This could happen only if $y_A^1 = 0$, that is, $\Omega = K_A$, which is a contradiction, or if $m_1 = \Omega/K_D$. The latter condition leads to a contradiction too, because for the solid state or a state across the wave to prevail inside the column it must be $m_1 \leq \Omega^2/(K_A K_D)$ (the sign = holding in the case of the state across the wave), and this upper bound is lower than Ω/K_D.

A similar analysis can be performed on section 4, leading to the same conclusion that the constant state consistent with the requirement of complete separation is the solid state constituted of pure desorbent and characterized by the same pair (K_B, K_A). It prevails inside the column provided that $m_4 \leq K_B/K_D$.

To obtain complete separation under robust operation the admittable ranges of the net flow rate ratios reported above, which have been obtained by applying the Equilibrium Theory, must be modified as follows: $m_1 > K_A/K_D$ and $m_4 < K_B/K_D$.

Sections 2 and 3: partial results

In the case of section 2, the solid state (Ω_1^γ, Ω_2^γ) and the fluid state (K_B, Ω_E) are separated by the intermediate state (K_B, Ω_2^γ) and they are connected by two transitions. The transition between the solid state and the intermediate state is a shock wave, because $\Omega_1^\gamma \geq K_B$. The character of the transition between the intermediate and the fluid states depends on whether Ω_2^γ is greater than Ω_E or vice-versa. In order to decide this, let us consider the situation when the state inside the column is the intermediate one and the corresponding material balance of component A at boundary A is Eq. 27. By using Eq. 25, the latter equation can be written in the Ω space as:

$$\frac{K_A - \Omega_2^\gamma}{\Omega_2^\gamma}\left(\frac{\Omega_2^\gamma}{K_D} - m_2\right) = (m_1 - m_2)\frac{K_A - \Omega_E}{\Omega_E}. \qquad \text{(C2)}$$

Let us assume $\Omega_2^\gamma > \Omega_E$. It follows that $(K_A - \Omega_2^\gamma)/\Omega_2^\gamma < (K_A - \Omega_E)/\Omega_E$ and that Ω_2^γ/K_D must be greater than m_1 for the relationship (Eq. C2) to be fulfilled. This is a condition on m_1 which is in contradiction with the constraint on this parameter derived above, namely $m_1 > K_A/K_D$. On the contrary if we assume $\Omega_2^\gamma < \Omega_E$, the two consistent inequalities $m_1 > K_A/K_D \geq \Omega_2^\gamma/K_D$ are obtained. It can be concluded that:

$$\Omega_2^\gamma < \Omega_E \qquad \text{(C3)}$$

and therefore the transition between the intermediate state and the fluid state is a simple wave.

The behavior of section 3 is analogous. The solid state (Ω_R^S, K_A) and the fluid state (Ω_1^β, Ω_2^β) are separated by the intermediate state (Ω_1^β, K_A) and they are connected by two transitions. The transition between the intermediate state and the fluid state is a shock wave, because $K_A \geq \Omega_2^\beta$. Furthermore it can be demonstrated as well as for section 2 that:

$$\Omega_R^S \leq \Omega_R < \Omega_1^\gamma \qquad \text{(C4)}$$

and therefore that the transition between the solid state and the intermediate state is a simple wave.

The net flow rate of the ith component in the jth section is proportional to the quantity f_i^j, given by $f_i^j = m_j y_i^j - \theta_i^j$. The requirement of complete separation imposes that the net flow rate of component B in section 2 be positive and that the net flow rate of component A in section 3 be negative. By using Eqs. 12, for component B in section 2 it can be written:

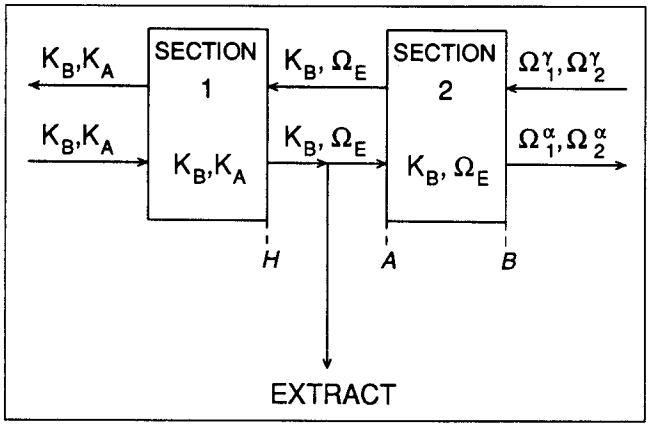

Figure 16. Sections 1 and 2, when the constant state prevailing inside section 2 is the fluid state.

$$f_B^2 = y_B^2\left(m_2 - \frac{\Omega_1^2\Omega_2^2}{K_A K_D}\right). \tag{C5}$$

It follows that the steady constant state cannot be the solid state, characterized by the pair $(\Omega_1^\gamma, \Omega_2^\gamma)$. In fact $m_1 \le \Omega_1^\gamma\Omega_2^\gamma/(K_AK_D)$ for the solid state to prevail inside the column, and if this condition held true, f_B^2 would be ≤ 0, so contradicting the above requirement. A similar reasoning can be followed to demonstrate that the steady constant state inside section 3 cannot be the fluid state $(\Omega_1^\beta, \Omega_2^\beta)$. In fact in this case—obtained with $m_3 \ge \Omega_1^\beta\Omega_2^\beta/(K_BK_D) - f_A^3$ for component A in section 3 is given by

$$f_A^3 = y_A^3\left(m_3 - \frac{\Omega_1^3\Omega_2^3}{K_B K_D}\right), \tag{C6}$$

hence it would be ≥ 0.

The other two extreme cases too can be discarded as possible steady constant states. If the steady constant state inside section 2 is the fluid state, m_2 must be $\ge (\Omega_E)^2/(K_AK_D)$. From theorem 1 it follows that the outgoing adsorbed state is also (K_B, Ω_E). The easiest way to demonstrate that this is not acceptable is to consider also section 1 and to show that the upper range regime in section 1 is not compatible with the configuration under examination. Let us write the material balance of component A at boundary H with reference to Figure 16. We obtain:

$$y_A^E = \mu_1[\epsilon_p y_A^E + (1-\epsilon_p)\sigma\theta_A^E], \tag{C7}$$

from which the condition $m_1 = \Omega_E/K_D$ is derived, which is not compatible with the regime imposed to section 1 in order to obtain complete separation. In the same way, it can be shown that in section 3 the solid state cannot be the one prevailing after the completion of the transient.

Sections 2 and 3: complete results

We are left with the problem of finding out the states prevailing inside sections 2 and 3 after the completion of the transient. In particular, we must determine the value of Ω_2 in section 2 and the value of Ω_1 in section 3. In order to do this, we must analyze the structure of the system of equations which can be written to determine the unknown Ω values. They are the same 12 equations written in section 5 (Eqs. 19 to 30), together with the material balance of component A at boundary B and that of component B at boundary C, necessary to determine Ω_2^α and Ω_1^β. Let us transform the obtained system as follows:

- Use Eqs. 19 to 22 to eliminate the external mass-flow rates.
- Include Eqs. 35 and 36 instead of Eqs. 27 and 28.
- Leave out Eqs. 23 to 26, which are necessary only to calculate Ω_E, Ω_E^S, Ω_R and Ω_R^S, and not to determine the other unknowns of the system.
- Use Eqs. 12 to write the system in terms of the relevant Ω values.

So doing, we obtain the following system written for convenience in implicit form (the indices i and k of the function g_{ik} mean that the corresponding equation is the material balance of component i at boundary k; and the semicolon separates the unknowns from the parameters within the list of arguments of each function):

$$g_{AA}(\Omega_2^2;\ m_2,\ m_3,\ \Omega_F) = 0$$

$$g_{BB}(\Omega_1^\alpha,\ \Omega_2^\alpha,\ \Omega_1^\gamma,\ \Omega_2^\gamma;\ m_2) = 0$$

$$g_{AB}(\Omega_1^\alpha,\ \Omega_2^\alpha,\ \Omega_1^\gamma,\ \Omega_2^\gamma,\ \Omega_2^2,\ m_2) = 0$$

$$g_{BD}(\Omega_1^3;\ m_2,\ m_3,\ \Omega_F) = 0$$

$$g_{AC}(\Omega_1^\beta,\ \Omega_2^\beta,\ \Omega_1^\gamma,\ \Omega_2^\gamma;\ m_3) = 0$$

$$g_{BC}(\Omega_1^\beta,\ \Omega_2^\beta,\ \Omega_1^\gamma,\ \Omega_2^\gamma,\ \Omega_1^3,\ m_3) = 0. \tag{C8}$$

These are six equations in eight unknowns, to which the two relationships that make it possible to determine the steady constant state inside sections 2 and 3 from the net flow rate ratios m_2 and m_3 and the composition of the two incoming streams must be added. They can be written as:

$$\Omega_2^2 = F_2(\Omega_1^\gamma,\ \Omega_2^\gamma;\ m_1,\ m_2,\ \Omega_F), \tag{C9}$$

$$\Omega_1^3 = F_1(\Omega_1^\beta,\ \Omega_2^\beta;\ m_3,\ m_4,\ \Omega_F), \tag{C10}$$

where F_1 and F_2 depend on Ω_F, m_1 and m_4 through Ω_E and Ω_R^S, respectively. The functions g_{ik} are differentiable functions over the entire domain of interest, whereas F_1 and F_2 are not. In fact they are well defined operators which carry with them all the information we need about the solution of the single section differential problem.

If the steady constant states inside the columns are the intermediate ones, then $\Omega_2^2 = \Omega_2^\gamma$ and $\Omega_1^3 = \Omega_1^\beta$ and the net flow rate ratios must fulfill the relevant constraints $\Omega_1^\gamma\Omega_2^\gamma/(K_AK_D) \le m_2 \le (\Omega_2^\gamma)^2/(K_AK_D)$ and $(\Omega_1^\beta)^2/(K_BK_D) \le m_3 \le \Omega_1^\beta\Omega_2^\beta/(K_BK_D)$. If we substitute the values for Ω_2^2 and Ω_1^3 in the system of Eqs. C8, we obtain a system of six equations and six unknowns which can be shown to have one and only one solution. It follows that the intermediate states are admittable states for complete separation to be obtained.

Now let us consider the case when a state across the simple

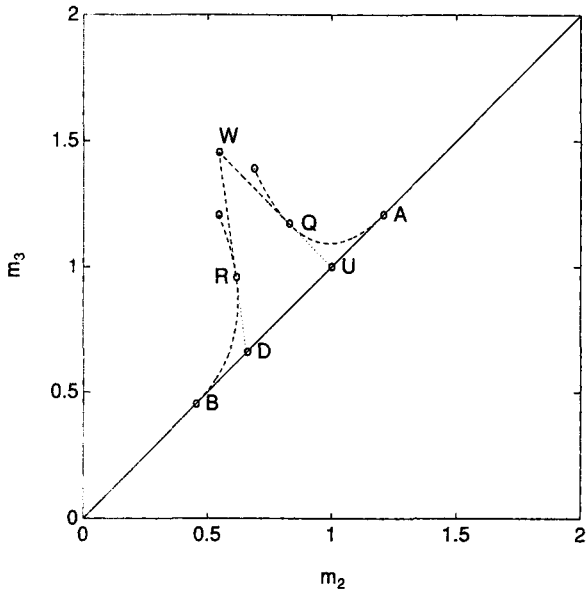

Figure 17. Region of complete separation in the $m_2 - m_3$ plane, including the points which are on the boundary of it.

wave between the intermediate and the fluid states or the intermediate and the solid state prevails inside section 2 or 3, respectively. In this case the operators F_2 and F_1 become continuous functions, namely $\Omega_2^2 = F_2(m_2) = \sqrt{K_A K_D m_2}$ and $\Omega_1^3 = F_1(m_3) = \sqrt{K_B K_D m_3}$. If we substitute these relationships into the equations $g_{AA} = 0$ and $g_{BD} = 0$, we obtain two relationships between m_2 and m_3, which constitute a pair of constraints on the operating parameters. In particular the equation $g_{AA} = 0$ implies that m_2 and m_3 be such that Eq. 67 holds true, whereas the equation $g_{BD} = 0$ implies that Eq. 68 is fulfilled. It can be easily shown that these two curves do not intersect, hence only one out of the two conditions can be valid. It follows that if a state across the simple wave prevails in section 2 or 3, the intermediate state must prevail in the other section. Then one of the two equations $g_{AA} = 0$ and $g_{BD} = 0$ becomes a relationship between m_2 and m_3 and does not belong to the system any more. The remaining five equations in six unknowns have infinite solutions, that is, one of the six unknowns can be chosen arbitrarily and the other five unknowns are obtained in terms of the first one. It can be demonstrated through an analysis along the lines of what is done in the sixth section that a subset of them fulfill all the constraints on m_2 and m_3 implied by the configuration of the four section unit under examination. Nevertheless, as shown in Figure 17, all these operating conditions correspond to points on the boundary of the complete separation set, that is, not internal points, hence they are not admittable as operating conditions to obtain complete separation under robust operation.

It follows that the only steady constant states in sections 2 and 3 consistent with the design requirement of complete separation are the intermediate states with constraints on the net flow rate ratios m_2 and m_3 as given in Table 1, to account for the requirement of robust operation. This completes the proof of theorem 1.

Appendix D

Optimal operating conditions

By summing up the two inequalities in Eqs. 60 and 61, it is readily seen that a necessary condition for complete separation is that $b_2 \geq b_1$, which using Eqs. 14, 39 and 40 yields:

$$(m_3 - m_2) \leq \frac{K_A - K_B}{K_A K_B} \Omega_F. \tag{D1}$$

This inequality, together with the constraint in Eq. 64 $(m_3 - m_2) > 0$, defines a band-shaped domain in the $m_2 - m_3$ plane. Since the optimal operating conditions correspond to maximum m_3 and minimum m_2, which implies that the difference $(m_3 - m_2)$ should be maximum, it follows that the optimal point belongs to the straight line of equation $b_2 = b_1$, which corresponds to the situation where the right- and left-hand sides of the inequality in Eq. D1 are equal.

By substituting $b_2 = b_1$ in Eqs. 60 and 61, it is found that at the optimal point also $c_2 = c_1$ must hold true, thus yielding:

$$m_3 = \frac{K_A}{K_B} m_2. \tag{D2}$$

Using Eqs. D1 and D2 the coordinates of the optimal point are the following: $m_2 = \Omega_F / K_A$ and $m_3 = \Omega_F / K_B$. It is worth noticing that, when the flow rate ratios are set at their optimal values, the adsorbed phase between sections 2 and 3 is at equilibrium with the feed stream. Accordingly the two streams share the same values of the Ω parameters, that is, Ω_F and K_D.

Region of complete separation

The five constraints given by Eqs. 60 to 64 determine the region of complete separation in the $m_2 - m_3$ plane. In the following, we further elaborate these conditions in order to identify the exact boundaries of such a region. The first one derives directly from the condition in Eq. 64 and corresponds to the straight line $m_3 = m_2$.

Now, let us consider Eqs. 62 and 63, which impose that the roots of Eqs. 38 and 37 be real. These can be written as: $|b_2| \geq 2\sqrt{c_2}$ and $|b_1| \geq 2\sqrt{c_1}$. Recalling that $b_1 > 0$ for any choice of m_2 and m_3 and $b_2 \geq b_1$, the modules in the above inequalities can be dropped, thus leading, through Eqs. 39 to 42 to the following constraints on the values of m_2 and m_3:

$$m_3 < m_2 + \frac{(\sqrt{K_A} - \sqrt{K_D m_2})^2}{y_A^F (K_A - K_D)}, \tag{D3}$$

$$m_2 > m_3 - \frac{(\sqrt{K_B} - \sqrt{K_D m_3})^2}{y_B^F (K_D - K_B)}. \tag{D4}$$

It can be readily seen that the curves corresponding to the boundaries of the above inequalities are tangent to the straight line $m_3 = m_2$ in the points A and B respectively, as defined by Eqs. 70 and 71. Moreover, the curves defined by Eqs. D3 and D4 go through the points Q and R defined by Eqs. 75 and 76, respectively. On the other hand, the coordinates of the optimal point W, given by Eq. 73, satisfy both inequalities. The bound-

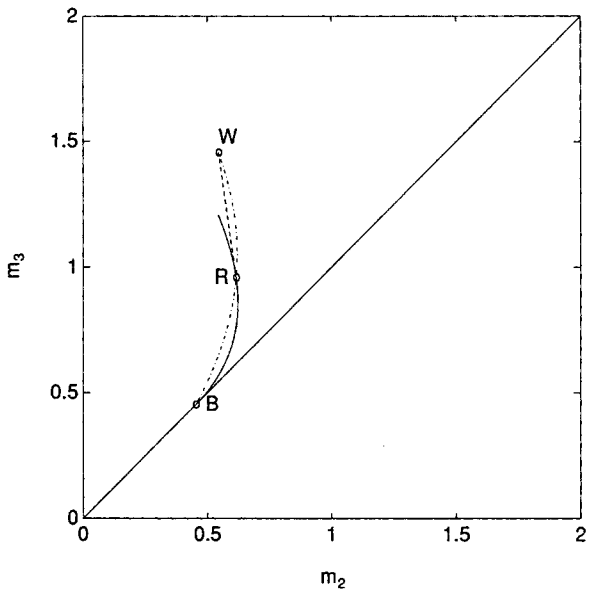

Figure 18. Construction of the complete separation region in the $m_2 - m_3$ plane by applying the conditions in Eqs. 60 to 64: — Eq. D4, —— Eq. D7, — • — Eq. D6.

aries defined by Eqs. D3 and D4, together with the straight line $m_3 = m_2$, are shown in Figure 17, where it can be seen that they do not identify a closed region. We should then proceed to consider the remaining conditions in Eqs. 60 and 61.

The condition in Eq. 60 can be rewritten as follows:

$$(b_2 - b_1)\sqrt{b_1^2 - 4c_1} \geq b_1(b_2 - b_1) + 2(c_1 - c_2). \qquad \text{(D5)}$$

This inequality is surely fulfilled in the region of m_2 and m_3 values where the righthand side is negative. Such a region is bounded by the following quadratic curve:

$$[K_D m_3 + K_B - y_B^F(K_D - K_B)(m_3 - m_2)] \times \left[K_A - K_B - \frac{K_A K_B}{\Omega_F}(m_3 - m_2)\right] + 2K_D(K_B m_3 - K_A m_2) = 0. \qquad \text{(D6)}$$

It is readily seen that this curve goes through the optimal point W, as well as through the points B and R (or S) defined by Eqs. 71 and 76 (or 77), respectively.

In the case where $\Omega_F < K_D$, using the operating conditions corresponding to the point R it can be seen that the root of Eq. 37 is given by $\Omega_1^{\ominus} = \Omega_F$. Similarly, in the case where $\Omega_F > K_D$, considering point S leads to $\Omega_1^{\ominus} = K_D$. Thus, in general we can state that for the operating conditions corresponding to the point where the curves defined by Eqs. D4 and D6 intersect (that is, R or S), we have $\Omega_1^{\ominus} = \min\{\Omega_F, K_D\}$, which is the same value corresponding to the optimal point, as mentioned above.

Thus summarizing, with reference to Figure 18, we have so far obtained the following results:

Below Point R or S. The separation region is on the righthand side of curve BR given by Eq. D4.

Above Point R or S. On the righthand side of the curve RW given by Eq. D6 complete separation is achieved. On the lefthand side of this curve, the righthand side of Eq. D5 is positive but nevertheless it can be smaller than the lefthand side of the same equation, which vanishes on the curve defined by Eq. D4. It follows that there must be another curve which is the boundary of the complete separation region and must pass through points W and R (or S). Its equation is given by Eq. D5, with the operator $=$ instead of the operator $\geq$. In other words, if a value of m_3 between point R (or S) and point W is fixed, for the corresponding point on the curve defined by Eq. D4 the inequality in Eq. D5 is not fulfilled because the lefthand side is zero, whereas the righthand side is positive. On the contrary, in the point with the same m_3 value but on the curve defined by Eq. D6 the inequality in Eq. D5 holds true, since the lefthand side is positive and the righthand side is zero. For continuity there must be a value of m_2 for which the left- and the righthand sides of Eq. D5 are equal. The points sharing this property when m_3 goes from its value in point R (or S) to the one in point W form the broken line RW shown in Figure 18.

Since in the points R or S $\Omega_1^{\ominus}$ has the same value as in the optimal point, corresponding to the maximum admittable value for Ω_1 according to theorem 2, we conjecture that the equation of the boundary that we are looking for is given by the relationship $\Omega_1^{\ominus} = \min\{\Omega_F, K_D\}$. We obtain:

When $\Omega_F < K_D$:

$$K_A(K_D - K_B)m_2 + K_B(K_A - K_D)m_3 = \Omega_F(K_A - K_B); \qquad \text{(D7)}$$

When $\Omega_F > K_D$:

$$y_B^F m_2 + y_A^F m_3 = 1. \qquad \text{(D8)}$$

Through straightforward but tedious algebra it can be shown that both the curves fulfill the equality in Eq. D5 and that they are tangent to the curve defined by Eq. D4 in point R and in point S, respectively.

A similar analysis can be performed using the condition in Eq. 61 to derive the remaining portion of the complete separation region boundaries, that is, the lines WT, WQ, QA and TA, whose expressions are reported by Eqs. 65 to 67.

Manuscript received May 8, 1992, and revision received Aug. 4, 1992.